University of Stavanger

Faculty of Science and Technology

MASTER'S THESIS

Study program/ Specialization: **Petroleum Engineering/** **Reservoir Engineering**	Spring semester, 2011 Open
Author: **Johan Helleren**	…… (Author's signature)
Faculty supervisor: **Dimitrios G. Hatzignatiou** External supervisor: **Arne Stavland**	
Title of thesis: **Numerical Simulation of Chemical Flow-Zone Isolation**	
Credits (ECTS): 30	
Keywords: Silicate Gel Gelation Time Reaction Rate Residence Time Retention History Matching Mobility Reduction Factor Residual Resistance Factor	Pages: 69 + Appendices: 5 Stavanger, 15th June 2011

ACKNOWLEDGEMENT

I would like to express my gratitude to several people that supported me during the last semester. First of all, I give my best thanks to Dimitrios Hatzignatiou as my supervisor for the support, guidance and enthusiasm during this thesis. I would also like to thank Arne Stavland at the International Research Institute of Stavanger (IRIS) for his assistance and guidance.

Thanks to all my fellow students and friends throughout my studies for some unforgettable moments. A special thanks to Jan Morten, Andreas, Fredrik and Sveta for their support and encouragement. Finally, thanks to my family for their support and keeping me motivated during all the good times and all the bad times.

TABLE OF CONTENTS

1 INTRODUCTION 1

1.1 BACKGROUND 1
1.2 SCOPE OF STUDY 1
1.3 OUTLINE 1

2 LITERATURE SURVEY RELATED TO UNWANTED FLUID PRODUCTION 2

2.1 ORIGINATE OF UNWANTED FLUID PRODUCTION 2
2.2 ISSUES WITH UNWANTED FLUID PRODUCTION 2
2.3 MEASURES TO DELAY PRODUCTION OF UNWANTED FLUID 3
2.4 ISOLATION OF PATHWAYS/WATER SHUT-OFF (WSO) 4
2.4.1 Disproportionate permeability reduction 4
2.5 TYPES OF GEL 5
2.5.1 Polymer gel 5
2.5.2 Other chemicals 5
2.6 SILICATE GEL 6
2.6.1 Chemistry of silicate gel 7
2.6.2 Effect of temperature and pH 9
2.7 FACTORS AFFECTING SILICATE/POLYMER GELATION 10
2.8 EXCESSIVE GAS PRODUCTION 13
2.9 DESIGN OF GEL 14

3 EXPERIMENTAL STUDY OF SILICATE GEL 15

3.1 BULK GELATION EXPERIMENT 16
3.1.1 Effect of salinity 16
3.1.2 Effect of pH and temperature 16
3.1.3 A gelation equation based on observed experimental data 17
3.2 DYNAMIC COREFLOOD EXPERIMENT 18
3.2.1 Core plugging time 18
3.3 STATIC COREFLOOD EXPERIMENT 20
3.3.1 Gel strength 20

4 STARS SIMULATOR GEL MODELLING CAPABILITIES 23

4.1 INTRODUCTION 23
4.2 CHEMICAL REACTION 23
4.2.1 Derivation of chemical reaction 23
4.2.1 Derivation of reaction rate 25
4.3 ADSORPTION/RETENTION 27
4.3.1 Critical concentration and critical gelation time 28
4.3.2 Calculation of gel concentration 29
4.3.3 Determine critical gel concentration 29
4.4 SENSITIVITY ANALYSES 31
4.4.1 Grid block analysis 31
4.4.2 Adsorption data analysis 32
4.4.3 Mol weight analysis 33

5 SIMULATION MODELS 35

5.1 DYNAMIC COREFLOOD EXPERIMENT 35
5.1.1 Reservoir description 35
5.1.2 Chemical reaction 35
5.1.3 Permeability data 36
5.1.4 Adsorption data 36
5.1.5 Injection design 36
5.2 STATIC COREFLOOD EXPERIMENT 37
5.2.1 Reservoir description 37
5.2.2 Chemical reaction 37
5.2.3 Permeability data 38
5.2.4 Adsorption data 38
5.2.5 Injection design 39

6 RESULT AND DISCUSSION 40

6.1 DYNAMIC COREFLOOD EXPERIMENT 40
6.1.1 Matching of relative effluent concentrations 40
6.1.2 Matching of differential pressure and liquid rate 44
6.1.3 Amount of gel reacted and adsorbed/retained 46
6.2 STATIC FLOODING EXPERIMENT 48
6.2.1 Injection of silicate solution – matching of RF 48
6.2.2 Shut-in period – amount of gel created 49
6.2.3 Post shut-in period (injection of water) – matching of RRF 51
6.3 DYNAMIC VERSUS STATIC COREFLOODING 53
6.4 CORE VERSUS RESERVOIR SCALE 53
6.5 MODEL LIMITATION 54

CONCLUSION 55

REFERENCES 57

NOMENCLATURE 60

APPENDIX 1 63

APPENDIX 2 65

APPENDIX 3 66

APPENDIX 4 67

LIST OF FIGURES

FIGURE 2-1: WATER CONING. 2
FIGURE 2-2: WSO APPLICATIONS IN RESERVOIR 4
FIGURE 2-3: SILICATE GEL. 6
FIGURE 2-4: POLYMERIZATION OF SILICATE 7
FIGURE 2-5: SILICATE STRUCTURE 8
FIGURE 2-6: STABILITY OF SILICATE 9
FIGURE 3-1: SAND COLUMN 15
FIGURE 3-2: GELATION TIME VERSUS HCL CONCENTRATION OBTAINED FROM EXPERIMENTAL DATA AND EQUATION 3.1. 17
FIGURE 3-3: INJECTION RATE AND DIFFERENTIAL PRESSURE IN THE DYNAMIC FLOOD EXPERIMENT #3 19
FIGURE 3-4: EFFLUENT CONCENTRATION IN THE DYNAMIC FLOOD EXPERIMENT #3. 19
FIGURE 3-5: EXPERIMENTAL AND MODELLED *RF* 21
FIGURE 3-6: EXPERIMENTAL AND MODELLED *RRF*. 22
FIGURE 4-1: GELATION TIME VERSUS HCL CONCENTRATION. 27
FIGURE 4-2: CRITICAL GEL CONCENTRATION VERSUS GELATION TIME FOR DYNAMIC COREFLOOD #3. 29
FIGURE 4-3: RELATIVE EFFLUENT CONCENTRATIONS AND GEL PRODUCED OBTAINED FROM SIMULATION RESULTS. 30
FIGURE 4-4: COMPARISON OF RELATIVE CONCENTRATIONS FOR VARIOUS AMOUNT OF GRID BLOCKS 31
FIGURE 4-5: COMPARISON OF DIFFERENTIAL PRESSURES WITH DIFFERENT *RRF*. 32
FIGURE 4-6: COMPARISON OF DIFFERENTIAL PRESSURE WITH DIFFERENT *ADRT*. 33
FIGURE 4-7: COMPARISON OF DIFFERENT SILICATE MOLECULAR WEIGHT. 34
FIGURE 4-8: GEL ADSORPTION WITH DIFFERENT ADSORPTION DATA. 34
FIGURE 5-1: ADSORPTION VERSUS GEL COMPOSITION IN THE CORE FOR THE DYNAMIC COREFLOOD. 36
FIGURE 5-2: MATCHING THE EXPERIMENTAL AND STARS GELATION TIME FOR THE INJECTION DESIGN IN THE STATIC COREFLOOD EXPERIMENT. 38
FIGURE 5-3: ADSORPTION VERSUS GEL COMPOSITION FOR THE STATIC COREFLOOD. 39
FIGURE 6-1: EFFLUENT CONCENTRATION VERSUS PV, EXPERIMENTAL AND SIMULATION. 40
FIGURE 6-2: ADSORBED GEL AT THE END OF FIRST INJECTION PERIOD. 41
FIGURE 6-3: ADSORBED GEL AT THE END OF THE SECOND INJECTION PERIOD. 42
FIGURE 6-4: ADSORBED GEL AT THE END OF THE THIRD INJECTION PERIOD. 43
FIGURE 6-5: DIFFERENTIAL PRESSURE AND INJECTED RATE VERSUS TIME, EXPERIMENTAL AND SIMULATION. 44
FIGURE 6-6: ADSORBED GEL AT RESIDENCE TIME = 13,6 DAYS. 45
FIGURE 6-7: GEL REACTED AND GEL ADSORBED VERSUS RESIDENCE TIME. 46
FIGURE 6-8: *RF* VERSUS FLUID INJECTED. 48
FIGURE 6-9: GEL IN THE CORE AFTER THE INJECTION OF SILICATE SOLUTION 49
FIGURE 6-10: GEL CONCENTRATION AND ADSORBED GEL VERSUS TIME. 50
FIGURE 6-11: GEL ADSORBED IN THE CORE AFTER 1,7 DAYS. 50
FIGURE 6-12: *RRF* VERSUS WATER INJECTED IN POST SHUT-IN 51
FIGURE 6-15: DIFFERENTIAL PRESSURE VERSUS FLUID INJECTED, CORRESPONDING TO THE *RRF* IN FIGURE 6-14 52

LIST OF TABLES

TABLE 3-1: GEL CODING. 16
TABLE 3-2: EFFECT OF CALCIUM CONCENTRATIONS. 16
TABLE 3-3: INJECTION DESIGN FOR THE DYNAMIC COREFLOOD. 18
TABLE 3-4: INJECTION DESIGN IN STATIC COREFLOOD EXPERIMENT. 20
TABLE 4-1: OVERVIEW OF KEYWORDS CONNECTED TO GEL MODELLING IN STARS 24
TABLE 4-2: OVERVIEW OF MASS FRACTIONS, CONCENTRATIONS AND ORDER OF REACTIONS. 26
TABLE 5-1: RESERVOIR DESCRIPTION IN DYNAMIC COREFLOOD EXPERIMENT #3. 35
TABLE 5-2: OVERVIEW OF MASS FRACTIONS, CONCENTRATIONS AND ORDER OF REACTIONS FROM DYNAMIC COREFLOOD #3. 35
TABLE 5-3: RESERVOIR DESCRIPTION IN STATIC COREFLOOD EXPERIMENT. 37
TABLE 5-4: OVERVIEW OF MASS FRACTIONS, CONCENTRATIONS AND ORDER OF REACTIONS FROM STATIC COREFLOOD. 37

Abstract

Silicate gel has been mostly used for near well treatment. A field test in the Snorre reservoir on the Norwegian Continental Shelf (NCS) has been planned, where the object of the test is to technically qualify silicate gel for deep placement. Compared with other types of gel, silicate gel is relative inexpensive, environmentally friendly and flexible.

The chemistry and polymerization process of silicate gels is complex. The silicate gel gelation time is affected by several parameters such as pH, temperature and concentration of the components. In order to optimize the silicate injection test planned in the Snorre reservoir, several experiments on silicate gel were conducted at the International Research Institute of Stavanger (IRIS). Bulk gelation, static and dynamic coreflood experiments were performed, with the aim of studying the kinetics and strength of the silicate gel. The experimental data obtained from the experiments were used to model the coreflood experiments to get a better understanding of the gel behaviour. The commercial numerical simulator, STARS was used for this purpose. Gel modelling capabilities in STARS is primarily based on a defined chemical reaction, and the adsorption/retention of a defined pure blocking gel.

The formation of gel in STARS is dictated by the chemical reaction implemented into the simulator and the reaction rate of the reactants. Gel modelling in STARS was not fully understood, since large amount of gel was created in the start of the run. To solve this issue, a critical gelation time and critical gel concentration terms were introduced, in order to reach the maximum gel adsorption level at the predetermined gelation time. The blocking effect in STARS is mainly controlled by the reduced water permeability factor *RKW*, which is primarily affected by the residual resistance factor *RRF*.

Dynamic coreflood and static coreflood were modelled to study the gelation time and the gel strength. In the dynamic coreflood, the relative effluent concentration and differential pressure were sampled during the experimental work. To be able to match the differential pressure, the *RRF* had to be adjusted at the plugging time of the core. The relative effluent concentration matched well with the data obtained from the simulation results at high injection rates. By changing the order of reaction of the reacting components, a better match can be obtained for the lower injection rates.

For the static coreflood the mobility reduction *RF*, and the residual resistance factor, *RRF* were sampled during the experimental work. A good match was obtained for the *RF*. To be able to match the *RRF*, connected with the differential pressure during the experiment, the adsorption had to be set as irreversible at $5000 < RRF < 20$, and reversible outside this range.

Utilising the STARS simulator gel creation and behaviour modelling capabilities it is possible to simulate and match silicate gel treatment results observed from various experimental coreflood runs.

1 Introduction

1.1 Background

In the recent years focus has been put on the use of silicate gels for flow zone isolation. The object of flow zone isolation is to reduce watercut and to enhance oil recovery. Polymers have mostly been used for this application, but silicates were suggested as plugging agents in water shut-off as early as the 1920's (Kennedy, 1936), and have been used to reduce water production in the petroleum industries since the 90's (Lakatos et al., 1999).

Sodium silicate was used in a field test for gel treatment in the producer well on Gullfaks, to improve oil recovery. The effect of the gel was studied by the use of the chemical simulator SCORPIO (Rolfsvåg et al., 1996). To technically qualify silicate gel for deep placement several experiments were executed at the International Research Institute of Stavanger (IRIS). Bulk gelation, dynamic and static corefloods experiments conducted, with the purpose of optimizing the design of the silicate to the test. Based on the experimental data, gelation kinetic parameters were established (Stavland, 2011).

1.2 Scope of study

The object of this thesis is to model the laboratory data obtained by Stavland et al., (2011). By studying the effect of parameters such as temperature, pH and concentration of the substances involved in the gelation process, the behaviour of the silicate gels in the porous media can be better understood. Two of the experiments were modelled; the static coreflood and the dynamic coreflood #3. In the static coreflood, the focus was on matching the mobility reduction *RF*, and the residual resistance factor *RRF*. For the dynamic coreflood the focus was on matching the relative concentrations of the effluents and the differential pressure during the experiment.

By modelling corefloods and history matching the simulation results with experimental data, a predictive tool could be developed on a core-scale level. For the numerical simulation study, there were three potential simulators to choose between; UTCHEM, STARS and ECLIPSE. After careful consideration of these simulators, the commercial simulator STARS (STARS, 2009), which have the capacity to model chemical reactions and gel treatments. From the literature survey, silicate gel has never earlier been simulated on STARS. The component data in the simulator was configured to be mass based. Also lab units were used in the simulator.

1.3 Outline

The focus in this thesis is on the silicate gel properties, not the enhanced oil recovery (EOR) capabilities. Initially, the unwanted fluid production issues are described, and measures are introduced, which can be implemented to solve these problems. A sensitivity analysis is also done, to get sufficient quality over the results obtained from the simulation.

2 Literature Survey Related to Unwanted Fluid Production

2.1 Originate of unwanted fluid production

Formation water occurs naturally in hydrocarbon-bearing reservoirs, and is distributed according to gravitational and capillary forces. When hydrocarbons are produced, the formation water will eventually make its way to the production wells and water will be produced. In wells were gas is not commercially producible, gas is seen as an unwanted fluid. The amount of unwanted fluid production increases as the fields becomes older. Enhanced oil recovery techniques such as gas and water injection also contribute to unwanted fluid production.

Excessive water and gas production causes several issues related to production, such as decreased oil production, increased cost and environmental problems. Factors that can provoke early water breakthrough are:

- Coning
- Natural fractures
- Faults
- Layers with high permeability

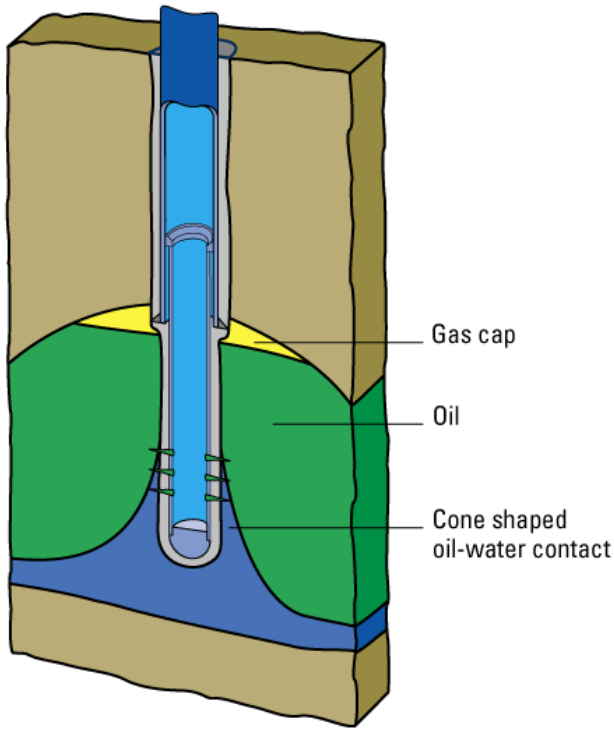

Figure 2-1: Water coning (Schlumberger, 2011).

2.2 Issues with unwanted fluid production

The production of unwanted fluids generates significant cost related to production of hydrocarbons. Early breakthrough of water or gas decreases the oil production, as the unwanted fluid is taking up space in the production facilities. Since water is heavier than oil, there can also be problems with production/lifting the hydrocarbons. The outcome might be that the well dies.

Measures that can be implemented to assist with reservoir fluids production are:

- Artificial lift: Production is improved by adding energy to the fluid column in the well. This can be done by implementing gas lift or a pump in the well.

- Gas lift: Gas is injected in the production tubing, with the aim of reducing the density of the fluid. The well can now be operated with higher flow rate, since the bottomhole pressure decreases.

Once water is produced, it can be injected into a new formation or back into the reservoir for enhanced oil recovery (EOR) purposes. The produced water contains minor parts of hydrocarbons, sand, metals and chemicals. To avoid issues with the produced water and the formation, such as plugging of pores and corrosion, it has to be treated, before injection. Therefore, it may not be profitable, because of cost related to the pretreatment.

Due to environmental regulation produced water can't be directly disposed into the sea offshore. The produced water contains substances, which can be harmful to the environment. Because of that, the produced water also has to be treated before it is discharged to sea, which increases the cost of produced water treatment further.

2.3 Measures to delay production of unwanted fluid

A way to decrease the amount of unwanted fluids and cost related to unwanted fluid production management is to delay the breakthrough of the unwanted fluids. The production of unwanted fluids can be delayed in several ways:

- Well type: By drilling horizontal wells, gas and water coning can be delayed. This is because a larger drainage area is obtained by a horizontal well, compared to a vertical well.
- Placement of well perforations: Design of type and location of well perforations (in cased wells) could also delay water and gas coning.
- Smart/intelligent wells: Well containing monitoring equipment and completion components that can be adjusted to optimize production. Production in layers can be adjusted, and turned off production in high watercut layers (Schiozer et al., 2009).
- Downhole fluid separation: The reservoir fluid is separated downhole. While the hydrocarbons are produced, the separated water is injected back into the reservoir or in a disposal well.
- Polymer injection: When water injection is used to enhance oil recovery, adding polymers to the water increases the viscosity and thereby reduces the mobility of the water. That way, the sweep efficiency is improved, and in addition to reduce the water mobility, viscous fingering is reduced.

2.4 Isolation of pathways/Water shut-off (WSO)

During production, fluid will flow fastest in the high permeable layers. Since the permeability in the reservoir often varies considerably in vertical direction, the contribution of water injection will be minor in the low permeable layers. Thereby, only a small fraction of the injected fluid will contribute as pressure support in these layers.

By isolation of pathways the breakthrough of water is delayed, in addition to enhance oil recovery. Isolating the high permeable layers, will forces the water to flow in the low permeable layers, and contribute to enhance oil recovery.

2.4.1 Disproportionate permeability reduction

Disproportionate permeability reduction (DPR) fluids have the ability to reduce the water permeability more than the oil permeability. A DPR fluid is usually a chemical that forms a gel in the pore space. The water injected after gelation, flow where the gel is weakest, most often along the pore wall (Grattoni et al., 2001).

In addition to gelation, the retention of the DPR fluid also contributes to permeability reduction. Usually the permeability reduction increases as the initial permeability decreases. To avoid this, the water saturation must be sufficient low to have open pathways for oil.

However, DPR fluids are also used for total blockage of pathways. Then both the water and oil permeability are significantly reduced. This application is usually used to shut-off high permeable layers with high watercut, and for casing repairs (Burns et al., 2008).

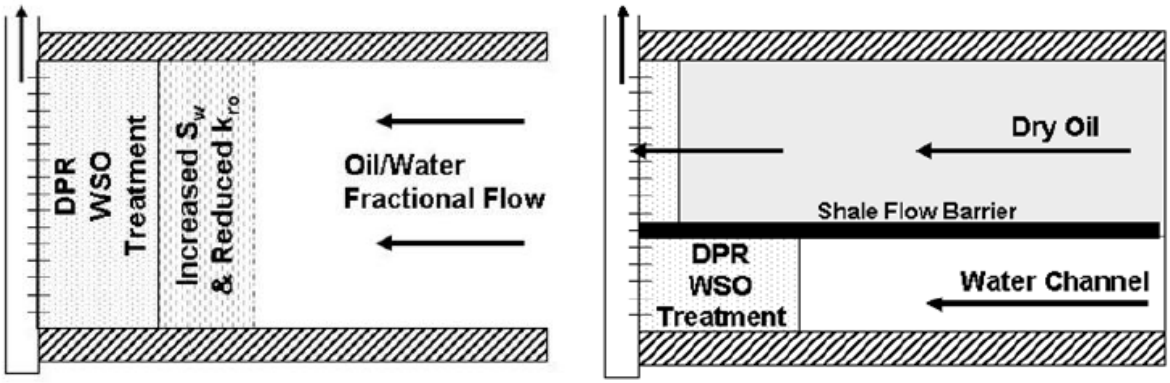

Figure 2-2: WSO applications in reservoir (Sydansk and Seright, 2006).

Figure 2-2 shows to the right a high permeable layer in the bottom, where water breakthrough has occurred. A WSO treatment is by that means applied in bottom layer, near the well. The illustration to the left has high watercut, and WSO treatment is applied near the well.

2.5 Types of gel

The types of gels available today are polymer gels, silicate gels and other chemicals (Kabir, 2001). Cement is most used for near wellbore treatments, because of difficulties with deep penetration and setting of the cement at reservoir conditions (Krumrine and Boyce, 1985).

2.5.1 Polymer gel

Polymer gels have mostly been used for water shut-off application, and can be used for both sealing and disproportionate permeability reduction. Polymers are mainly macromolecules, which are linked together by crosslinkers. Crosslinkers may be metal ions or metallic complexes. When crosslinked polymers are applied, polymers and crosslinking agent are injected into the reservoir, where a viscous gel is formed when these two components react. The polymers most used for water shut-off applications are:

- Polyacrylamides (PAM): PAM have good abilities of plugging of pores or fissures, because of its viscosity and gel strength.
- Biopolymers. Biopolymers have the ability to form physical network above critical concentration. As a result of the limited strength, they are not suitable for fracture treatment. They are more suited to plug of pores or fissures.

There are also ungelled polymers/viscous systems, which have the ability to reduce the water permeability more than the oil permeability. The advantages with these systems are that they can be bullheaded into an un-fractured well without zonal isolation. On the other hand, they are not strong enough to seal vugs and big voids, and there is also a risk of reducing the oil permeability. General issues with polymers are gelation control, adsorption and deep penetration, because of the viscosity. Due to the cost and technical aspect of polymers, it is mainly used for near wellbore treatment.

2.5.2 Other chemicals

- Inorganic gels: Inorganic gels are mostly used for plugging lost circulation, zone squeezing and consolidating weak formations. Generally, inorganic chemicals are used, which can be easily injected in the reservoir since the chemicals used are water thin. An activator is used to make the fluid gel. The disadvantages of inorganic gels are short gel time, low strength and that it reacts with acid and the formation. On the other hand it is cheap and can be used for deep penetrating, due to low viscosity of the fluid.
- Resin/Elastomers: Phenolic, Epoxy, and Furfuryl alcohol are typical thermosetting resins. The physical strength of resins makes them adequate to seal fractures, vugs, channels and perforations. However, they are relative expensive.
- Monomer based system: Monomer based system are suitable for deep penetration, because of their low viscosity. The issue is however to control the gelation time.

2.6 Silicate gel

Silicate gel can be used in water control and near well applications. According to Lakatos et al. (1999) the advantages of silicate well treatment can be summarized:

- *Candidate for deep penetration, because of low initial viscosity*
- *Inexpensive*
- *Environmental friendly*
- *Good thermal and chemical stability*
- *Easy to remove in case of any failures*

The disadvantages of silicate gel are the blocking effect and the gelation mechanisms. The silicate gel tends to shrink during time. An outcome of the shrinkage, is reduced blocking effect of the gel.

The other issue is the gelation time of the silicate gel. The gelation of silicate is an interaction of pH, temperature and concentrations of the reacting components. The gelation time might be difficult to control as the mechanisms of is not fully understood. The effect of these factors will be described later in chapter 3.

Figure 2-3: Silicate gel.

2.6.1 Chemistry of silicate gel

The polymerization, which is the process where the silicate increase in molecular weight, occurs in three simultaneous stags:

- *condensation of monomer and dimmer silicate species to form particles*
- *growth of particles*
- *linking of individual particles to form chains and subsequent networks, to form microgel*

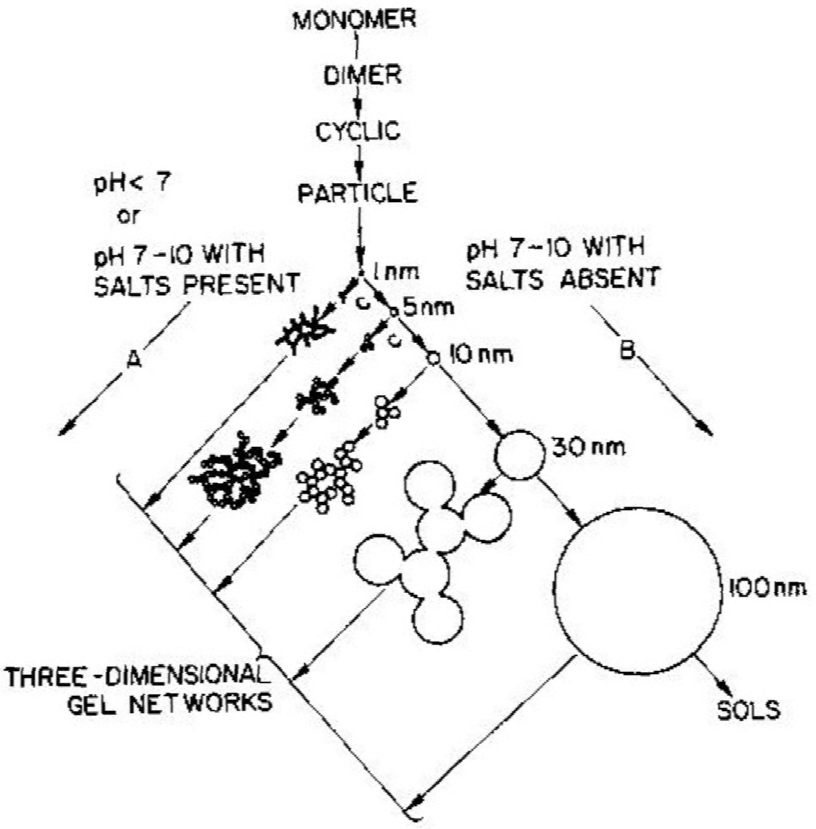

Figure 2-4: Polymerization of silicate (Iler, 1979).

In figure 2-4 the polymerization of silicate is shown. The polymerization is affected by salinity and pH. In solutions with little acid and salinity present (B), particles grow in size as the amount of particles decreases. In present of salt and acid (A), the particles aggregate into three-dimensional networks and form gels.

The chemistry of silicates is not completely understood, but according to Iler (1979) the following equilibria are involved:

$$SiO_2 + 2H_2O = Si(OH)_4$$
$$Si(OH)_4 + OH^- = HSiO_3^- + 2H_2O$$
$$2HSiO_3^- = Si_2O_5^{2-} + H_2O$$
$$Si_2O_5^{2-} + H_2O = HSi_2O_6^{3-} + H^+$$
$$HSiO_3^- + OH^- = SiO_3^{2-} + H_2O$$

When the concentration of $Si(OH)_4$ is above 100-200 ppm in an aqueous solution, and at the same time with no solid phase present, monomer and dimmer silicate condense to particles. If the concentration of $Si(OH)_4$ is less than 100 ppm, the solution is stable and soluble.

In the initial phase of the polymerization of silicates, ring structures are formed. These ring structures are thereby linked together by $Si(OH)_4$, and larger three dimensional molecules are formed. Often the Silicic acid grows in such way that there is a maximum of Siloxane (Si-O-Si) and minimum of uncondensed SiOH groups. Structure of the silicate is shown in figure 2-5. The size of the particle plays an important role for the gelation, because the smaller the particles are, the more soluble the particles are. For that reason, the smaller particles will dissolve, especially when the particle size is smaller than 5 nm. The outcome is that the particles grow in average size, and the number of particles decreases.

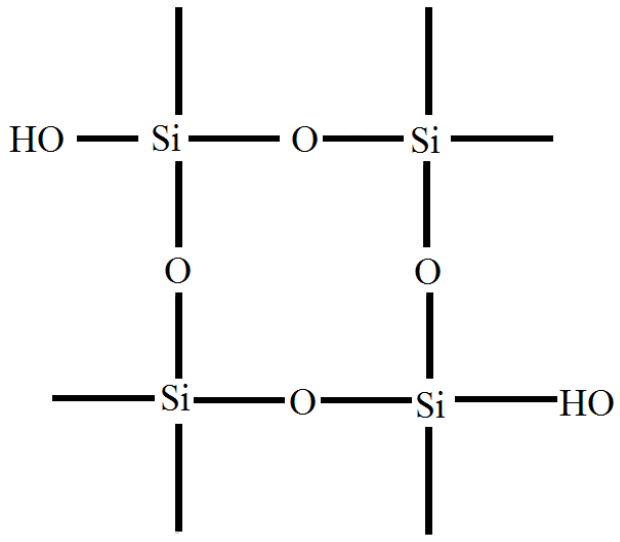

Figure 2-5: Silicate structure (eCompound.com, 2011).

2.6.2 Effect of temperature and pH

The temperature and pH is essential for the solubility of the particles, and with a pH above 7, dissolution and deposition is high. The particles grow until diameter reaches 5-10 nm, and after that the growth is slow. The silica particles are negatively charged above 6-7 pH to 10,5 and repel each other. The particles thereby grow in size. At high temperatures growth continues to larger particles. At low pH polymerization is slower. Figure 2-6 shows how the pH affects the stability of silicate. When salt is present, gelling occurs because of the decrease in charge repulsion, illustrated in figure 2-4. In some occasions the gelling is delayed by decreasing the temperature.

When the pH of the silicate is reduced, it can gel up by polymerization of the silicate. The speed of the reaction is because of that controlled by pH, which also affects the placement of the gel. To reduce the pH of the silicate, acid is added to the silicate solution.

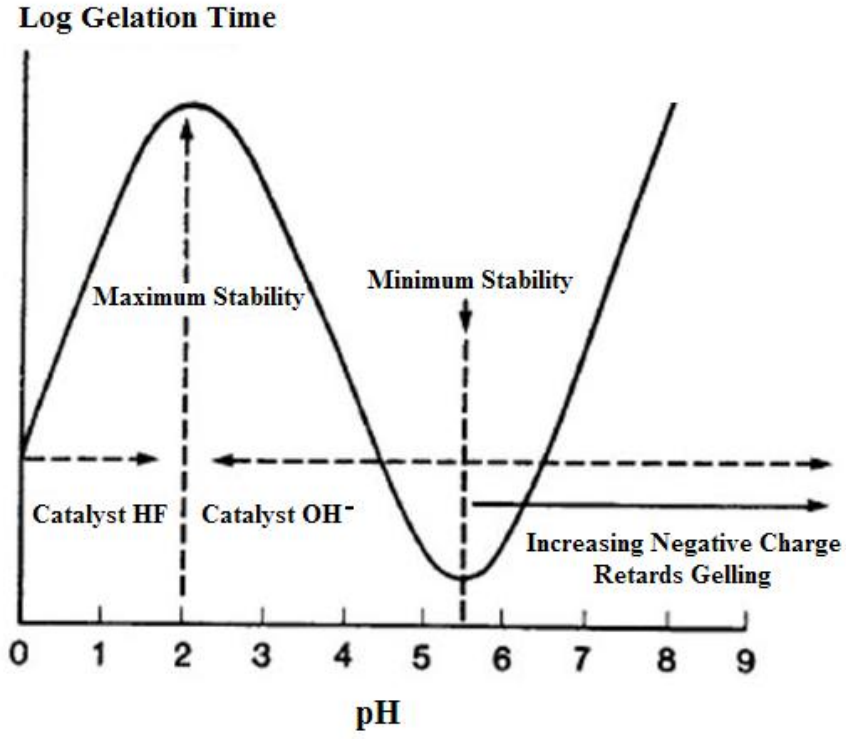

Figure 2-6: Stability of silicate (Vinot et al., 1989).

2.7 Factors affecting silicate/polymer gelation

To avoid issues with the gel treatment, it is important to be aware of the gel kinetics, and the factors affecting the behavior of the gel. The factors that influence the gelation most are:

- Reservoir type
- Gel system
- Gelation time
- Reaction rate
- Residence time
- Retention
- Dispersion
- Injection rate

Reservoir type: Gels are most successively applied in multilayered reservoir with different permeability. This setting causes earlier water breakthrough in high permeable layers. Therefore, gel treatment is mostly used in injection wells, but it is also applied in production wells to avoid coning.

Gel system: As mentioned earlier there are several types of gels available for isolation of pathways. The silicate/polymer consists mainly of three components; base material, reactants and an accelerator. The base material forms the matrix. The substances used depend on the type of gel that is applied. Basically, the base material determines the strength of the gel structure and ability of injection. Reactants are the component that makes the solution gel. The accelerator is used to control the gelation time.

Gelation time: The time it takes for the injected solution to gel (when viscosity starts to increase) after it is injected is called gelation time. The gelation time depends on the reaction rate of the gel.

Reaction rate: The reaction rate is the speed of the reaction. In a rate expression: C_1 + C_2 → products, the reaction rate is given by:

$$r_k = k \prod_{i=1}^{n_c} [C_i]^{e_k} \qquad (2.1)$$

r_k: Reaction rate [kg/(min·cm^3)]
k: Rate constant [1/min]
C_i: Concentrations of reactants [kg/cm^3]
e_k: Order of reaction [-]

The reaction rate is affected by the concentration of the reactants and the order of reactions. A reaction occurs mainly because of collisions between the molecules of the reactants. Increasing the concentrations of reactants would result in more collisions of molecules and thereby a faster reaction is obtained.

The order of reaction is the power of the reactant C_i, which express the contribution of the component C_i in the reaction. The order of reaction varies from 0, 1, 2, … An order of reaction equal to 0 means that the reaction is not affected by the concentration of the corresponding component. The order of reaction is found by experimental work (Masterton and Hurley, 2004).

An activation energy is required to make the collisions between molecules effective. The majority of reactions are increased as the temperature is increasing. The molecules obtain higher energy and speed with higher temperature, and thereby more molecules collide and react. For a temperature dependant reaction the rate constant is given by the Arrhenius equation:

$$k = r_{rk} \cdot e^{-E_a/RT} \tag{2.2}$$

r_{rk}: Frequency factor [1/min]
E_a: Activation energy [J/mole]
R: Molar gas constant [8,3145 J / (^{o}K·mole)]
T: Temperature [^{o}K]

The frequency factor is the frequency of collisions between the molecules. It is determined by experimental work.

Substituting equation (2.1) into equation (2.2), the following expressions is derived for the reaction rate:

$$r_k = r_{rk} \cdot e^{-E_a/RT} \prod_{i=1}^{n_c} [C_i]^{e_k} \tag{2.3}$$

Equation 2.3 is equation used in STARS simulator to model the creation of gel.

Factors that affect the gelation time in addition to concentration of components and temperature are the salinity and pH of the formation water. Generally, gelation time decreases with increasing base material concentration, reactants concentration, temperature and molecular weight (Green and Willhite, 1998).

Residence time: Residence time is the duration the fluid remains in the in the core, before it is eventually produced. Injection rate is given by:

$$q_{inj} = \frac{V_{pore}}{t_{res}} = \frac{\phi_f \cdot l \cdot Area}{t_{res}} \tag{2.4}$$

q_{inj} : Injection rate [ml/min]
ϕ_f: fluid porosity [-]
V_{pore}: Pore volume [ml]
t_{res} : Residence time [min]
l: Length of core [cm]
Area: Cross-sectional area of core [cm^2]

By rearranging equation (2.4), the following expression for residence time is derived:

$$t_{res} = \frac{\phi_f \cdot l \cdot Area}{q_{inj}} \tag{2.5}$$

Too short residence time may result in a gel that is not fully formed, which affects the strength and blocking effect of the gel.

Retention: The residence time increases as the injection rate decreases. With increasing residence time, particles grow in size. Thereby, more particles get accumulated in the pore throats. As more and more particles get retained in the core, the permeability of the core reduces (Nabzar et al., 1996).

The mobility reduction after a DPR fluid flow is given the mobility reduction factor *RF*,

$$RF = \frac{k_w \mu_p}{k_p \mu_w} \tag{2.6}$$

RF: Mobility reduction [-]
k_w : Effective water permeability [mD]
k_p : Effective polymer permeability [mD]
μ_w : Water viscosity [cP]
μ_p : Silicate/polymer viscosity [cP]

The permeability reduction is given by the residual resistance factor *RRF*:

$$RRF = \frac{\lambda_{before}}{\lambda_{after}} \tag{2.7}$$

RRF: Residual resistance factor [-]

λ_{before} : Mobility before DPR fluid flow [mD/cP]

λ_{after} : Mobility after DPR fluid flow [mD/cP]

Dispersion: When fluid is injected into the formation, mixing occurs between the displaced and displacing fluids. In other words, there is dispersion between the fluids. As the injected fluid moves through the reservoir, it gets more and more diluted. Dispersion is very important regarding the size of the DPR solution injected in order to get total blockage of the pores (Green and Willhite, 1998).

Injection rate: The silicate/polymer solution is bullhead injected into the formation, i.e. injected without any isolation of layers. The injection rate must be sufficient enough to get the fluid into the reservoir, but lower than the fracture pressure.

2.8 Excessive gas production

For excessive gas production, foam is often used to delay the breakthrough of gas and as an EOR agent. Foam is gas mixed with liquid containing minor amount of foaming agents (Green and Willhite, 1998).

Foam can be used as:

- Blocking of unwanted fluids, such as the coning of gas or water in production wells.
- Blocking of injected fluids in high permeable layers or fractures.
- Reducing the mobility of the injected phase, in order to improve the sweep efficiency.

Gels can also be used for delay of excessive gas, but due to the mobility of gas it may be difficult.

2.9 Design of gel

The gelation time is the most critical factor connected to the effect of the gel treatment, since the placement of the gel is mostly based on the gelation time. Too short gelation time can cause the settling of the gel in a different place than planned in advance. Nevertheless, too short residence time may result in a gel that is not fully formed, which affects the strength and blocking effect of the gel.

The design of the gel is important, in order to make the gel treatment effectively. Taking the gelation factors (cf. 2.7) into consideration, issues such as too early gelation, low gel strength and too small gel size can be avoided. The effect of these factors can be studied in experimental lab work.

Based on experimental lab work, a numerical simulation study can be done to develop a predictive tool. Thereby, the behavior of the gel can be predicted and understood better. The simulation results are then analyzed and parameters are tuned to optimize the design of the gel (Herbas et al., 2004).

3 Experimental Study of Silicate Gel

Several experiments were performed on silicate gel at the International Research Institute of Stavanger (IRIS). The purpose of these experiments was to optimize the design of the silicate used for the silicate injection test planned in the Snorre reservoir on the NCS. The object of the injection test at Snorre is to technically qualify silicate as a diversion agent. Three types of experiments were performed; bulk gelation, dynamic and static coreflood. During the experiments the effect of pH, temperature, concentration of silicates, gelation kinetics and gel strength were studied (Stavland et al., 2011). To produce similar residence time as in the planned field test, the injection rates were adjusted accordingly. The flooding experiments were performed in long sand columns, with the purpose of mimicking deep placement of gel. The sand columns were saturated with 100% water, which contained multi pressure ports, to observe the placement of the gel.

Sodium silicate, $(SiO_2)_n$:Na_2O was used in the silicate experiment, which had a pH of 11-13. The ratio between $Si(OH)_2$ and Na_2O affects the alkalinity of the system, i.e. how much acid/base the system can tolerate before the pH value changes. A low ratio would indicate a system that can tolerate significant amounts of acid in order to gel. In this case the ratio, n was equal to 3,4. Hydrochloric acid was used as accelerator to control the pH value of the silicate solution. The sodium silicate, which also contained 170 ppm of aluminium ions, was diluted in water that contained 20 ppm concentration of calcium.

Chemical reactions between reservoir minerals and sodium silicate where also studied by mixing sodium silicate with formation brine containing divalent cations. Precipitation of $Mg(OH)_2$ can occur when these components are mixed, and to avoid this issue the formation has to be pre-flushed. Flooding experiments were executed to determine size of the pre-flush needed. Sand columns saturated with different salinity of formation water were used in the experiments. By injecting silicate solution *RRF* and *RF* were studied. It was found that the permeability of the sand cores is reduced as the salinity of the formation water is increased.

Figure 3-1: Sand column (Lei et al., 2010).

3.1 Bulk gelation experiment

Bulk gelation experiments were performed to study how the gelation time changed, by modifying factors such as the temperature, pH, salinity and concentrations of the injected chemicals. The gel was inspected visually, to determine the degree of gelation. Table 3-1 describes the coding of the gel context. In order to study the plugging effect, filtration experiments were performed through a 3 μm filter. Plugging of the filter was observed when the gel reached code 1.

Table 3-1: Gel coding.

Gel code	Description
0	Clear and low viscous fluid
1	Cloudy and low viscous fluid
2	Cloudy and high viscous fluid
3	Rigid gel

3.1.1 Effect of salinity

The brine salinity affects the gelation time, as it decreases when the NaCl concentration of the makeup water was increased. The same trend was observed when the calcium concentration was increased. Calcium is not directly involved in the gelation process, but affects the gelation rate, as calcium ions are exchanged (Stavland, 2011). An overview of the gelation time at various calcium contents is shown in table 3-2. At small amount of calcium, the gelation time is significant higher compared to when high amount of calcium is added.

Table 3-2: Effect of calcium concentrations.

Ca^{2+} [ppm]	Gelation time, t_{gel} [days], T=40 ^{o}C	Gelation time, t_{gel} [days], T=60 ^{o}C
156,0	1,86	0,69
52,0	3,00	0,83
15,6	5,87	1,74

3.1.2 Effect of pH and temperature

It was found that small variations in pH had large effect on the gelation time. However, it was difficult to control the pH. Therefore, it would be more convenient to use hydrochloride to control the gelation time.

The experimental data also showed that the gelation time decreased as the temperature increased. For temperature dependency chemical reactions, the Arrhenius equation is normally used. The average activation energy for the gel reaction was found to be 77000 J/mol during the experiments.

3.1.3 A gelation time equation based on observed experimental data

Based on the experimental data an equation for gelation time was derived (Stavland et al., 2011):

$$t_{gel} = A \cdot e^{\alpha[Si]} \cdot e^{\beta[HCl]} \cdot e^{\gamma[Ca^{2+}]} \cdot e^{\frac{E_a}{RT}} \tag{3.1}$$

t_{gel}: Gelation time [days]
Si: Silicate concentration [wt%]
Ca^{2+}: Calcium concentration [ppm]
HCl: Hydrochloric acid concentration [wt%]
A = Gelation time tuning parameter [-]
α = -0,6 [1/wt%]
β = -0,7 [1/wt%]
γ = -0,1 [1/wt%]
E_a = 77000 [J/mole]

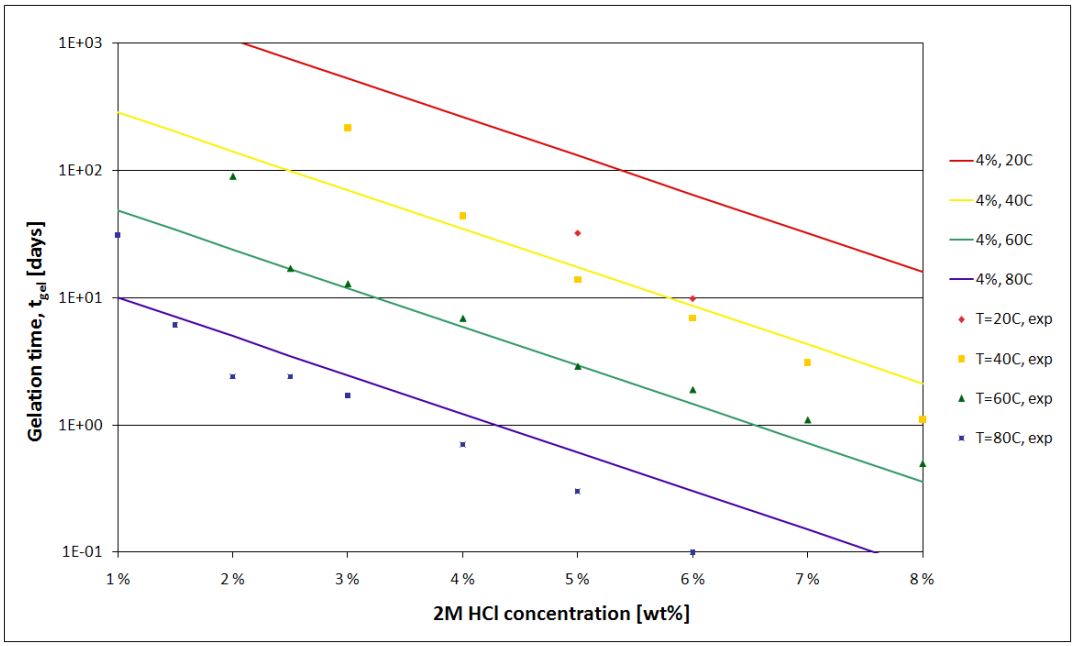

Figure 3-2: Gelation time versus HCl concentration obtained from experimental data and equation 3.1.

Figure 3-2 shows the gelation time for 4 wt% silicate and 20 ppm calcium and gelation time based on equation 3.1, at various temperatures. The solid lines are the gelation time from the equation 3.1, while the dots are the gelation time from experimental data. The colour blue represent temperature equal to 80°C, green is temperature equal to 60°C, yellow corresponds to temperature equal to 40°C and red denotes temperature equal to 20°C. The gelation time equation matches well with the experimental data obtained at temperature range 40-60°C, in figure 3-2. For temperature equal to 20°C it does not match, and for 80°C it matches the experimental data at low HCl concentrations.

3.2 Dynamic coreflood experiment

The dynamical flood experiments were performed by continuously injection of silicate solution through three sand columns, which had a length of 75 cm each. The three sand columns were coupled together and had a pore volume of 2100 ml, and contain six different pressure sections. The permeability and porosity of the core were 9000 mD and 41%. The silicate solution was premixed before injection, due to the low injection rate. The low injection rate was used to get a residence time of several days. The injection designs of the experiments are described in table 3-3.

Table 3-3: Injection design for the dynamic coreflood.

Experiment	**#1**	**#2**	**#3**
Si [wt%]	4,00	4,00	4,00
2 M HCl [wt%]	4,76	6,50	4,76
Al^{3+} [ppm]	170	170	170
Ca^{2+} [ppm]	20	20	20
Temperature [^oC]	55 and 64	55	55
Residence time, t_{res} [days]	6,13	6,07	0,04-17,10
Injection rate [ml/min]	0,24	0,24	11,70-0,03

For experiments #1 and #2 a constant injection rate was used. In experiment #3, the injection rate varied and only one of the three sand columns were used, in order to study the effect of blocking versus injection rate. Also the relative concentrations of the effluent were sampled, which is:

C/C_0: effluent concentration/initial concentration [-] (3.2)

3.2.1 Core plugging time

During the first experiment no blocking was observed during the first 7 days. In order increase the gelation, the temperature was increased to 64^{o}C. After 13,5 days, blocking occurred in the last section of the core. The designed plugging time was 3,2 days. The main reason for the delay was high permeable sand. During the bulk gelation experiments gel blocked a 3 µm filter. 9000 mD corresponds to a 8 µm filter. The ratio between designed and actual blocking time was 3,6.

In the second experiment it was assumed that the blocking would occur 3,6 times later than predicted. Blocking occurred after 4,6 days in the last section of the core.

In the third experiment the injection rate varied from 11,7 ml/min to 0,03 ml/min shown in figure 3-3. While the designed gelation time was 11,6 days, the residence time of the silicate solution injected with a rate above 0,03 ml/min, would be lower than the gelation time. Thereby, the core would not be plugged until 11,6 days. The plugging was observed at 13,6 days, when the pressure significantly increased in the last section, which can be seen in figure 3-3.

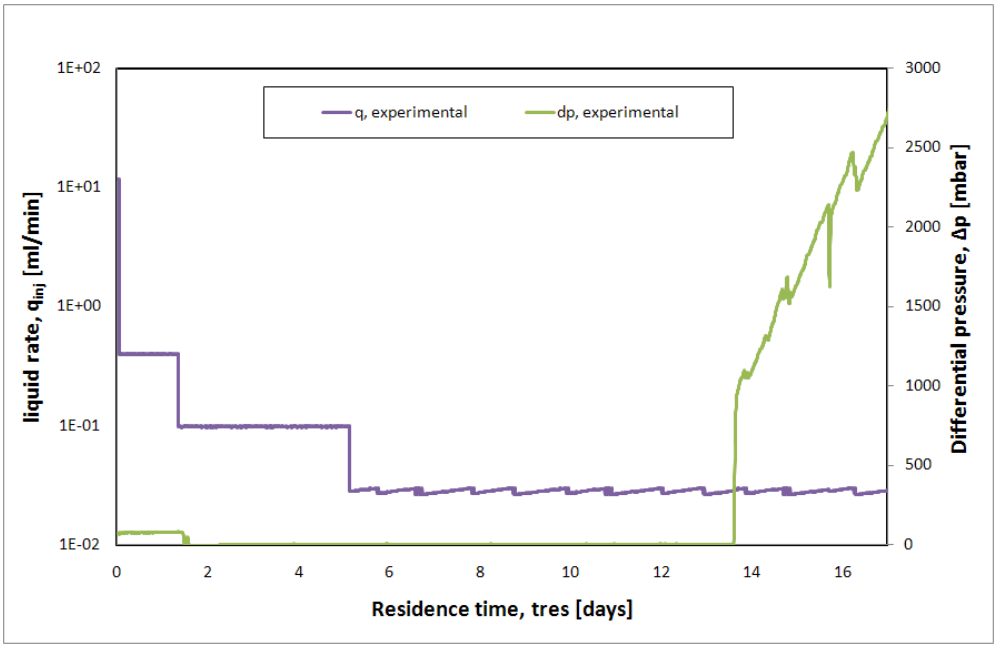

Figure 3-3: Injection rate and differential pressure in the dynamic flood experiment #3.

In experiment #3 the relative concentrations of effluents were sampled. The experimental data is shown in figure 3-4, where the solid blue line is the residence time, the brown round dots are calcium, the black triangular points are aluminium, the green dots are silicate and the orange triangular are relative OH^-. It was found that around breakthrough of the silicate solution, at 1 pore volume fluid injected, the relative concentration of calcium and silicate was close to 1. The retention of silicate was low at this time. When the residence time increased, the retention started to increase. Because of plugging of the back pressure regulator during the end of the experiment, it was not possible to monitor the effluent after 5 pore volumes fluid injected.

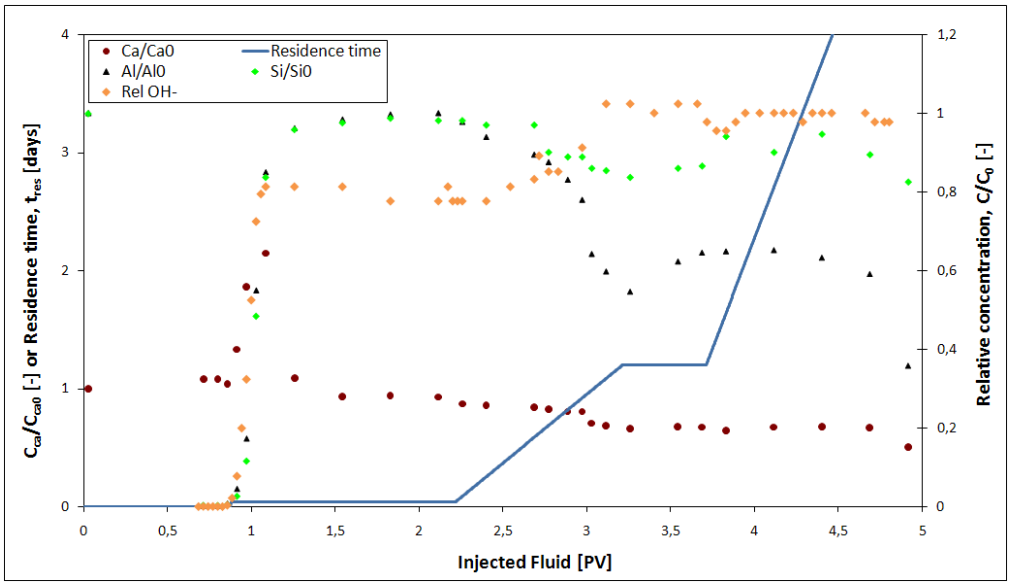

Figure 3-4: Effluent concentration in the dynamic flood experiment #3.

3.3 Static coreflood experiment

To study the gel strength of the silicate gel, a static coreflood experiment with shut-in of the core was performed. The length of the sand column was 30,3 cm, and had a diameter and porosity that corresponds to a pore volume of 80 ml. The permeability of the sand column was 8000 mD. A silicate solution with the design described in table 3-4 and a viscosity of 1,19 cP, was injected into the sand column, with a temperature of 40^{o}C. The experiment was divided into three periods; injection of silicate solution, shut-in and post shut-in. During the first period, 5 pore volumes of silicate solution were injected with a rate equal to 5 ml/min. The sand column was then shut-in for twelve days, so that gel would form. With the given injection design in table 3-2 the gelation time was calculated with equation 3.1, to be 1,7 days (cf. Appendix 2). As the residence time was lower than gelation time for the silicate, no gel should be formed during the first period.

With the purpose to study the strength of the silicate gel, water was injected with a rate equal to 0,05 ml/min into the sand column until a stable mobility reduction was observed in the post shut-in period.

Table 3-4: Injection design in static coreflood experiment.

Si [wt%]	3,0
2 M HCl [wt%]	8,5
Al^{3+} [ppm]	31,0
Ca^{2+}[ppm]	20,0

3.3.1 Gel strength

During the static coreflood experiment, the mobility reduction, *RF* and the permeability reduction, *RRF* were monitored and the RF and RRF models were developed as followed (Stavland et al., 2011):

$$RF = RF_g + \frac{RF_g - RF_d}{1 - x} \text{ for } x < 1 \quad (3.3)$$

$$RF = RF_d \text{ for } x > 1 \quad (3.4)$$

RF_g: Initial mobility reduction [-]

RF_d: Final mobility reduction [-]

x: Relative front position of the degradation front [-]

The expression for the effective permeability reduction:

$$RRF = (1-x)RRF_g + xRRF_d \text{ for x < 1} \quad (3.5)$$

$$RRF = RRF_d \text{ for x > 1} \quad (3.6)$$

RRF_g: Initial permeability reduction [-]
RRF_d: Final permeability reduction [-]

In figure 3-5 the blue dots are the experimental *RF* and the solid black is the modelled *RF*. The *RF* is plotted until 5 pore volumes fluid injected, and the *RF* continuously increases until breakthrough of the silicate solution at 1 pore volume. Since the designed gelation time was 1,7 days, the permeability would not be modified. However, the effect of the increased silicate viscosity would explain the increase in *RF*, based on equation 2.6. Initially, the core is 100% water saturated, and the viscosity of the fluid in the core increases until the silicate solution has flown through the core. The experimental data deviates slightly from the modelled *RF*, and increases to 1,23 at 4 pore volumes fluid injected.

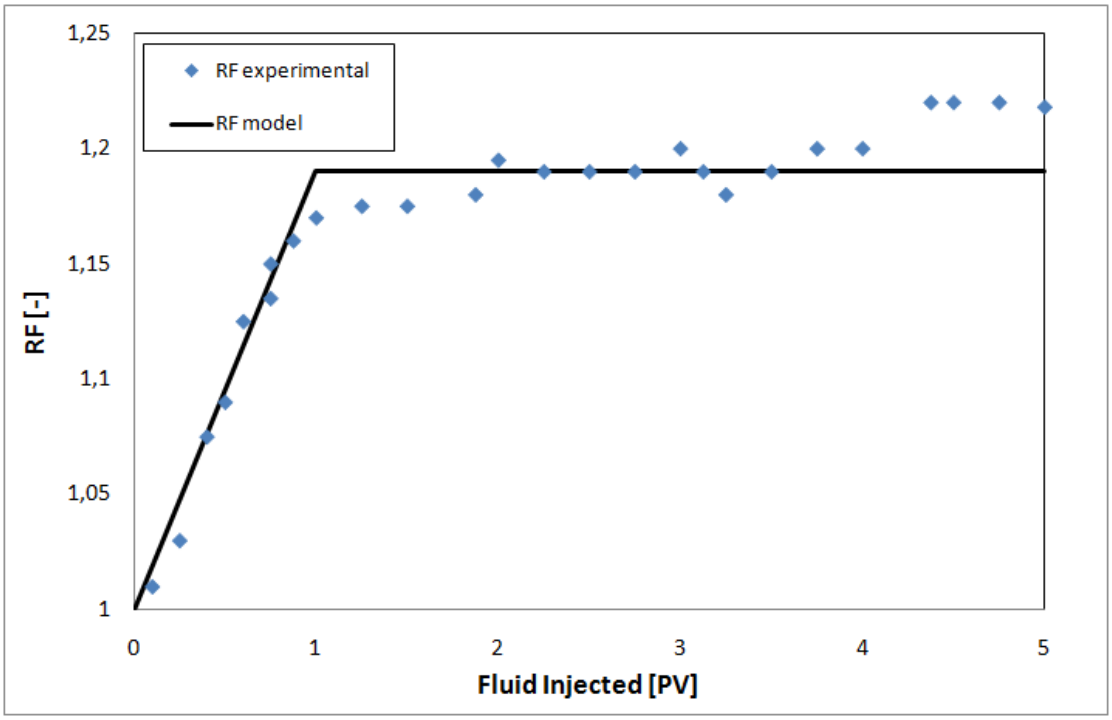

Figure 3-5: Experimental and modelled *RF*.

To make the silicate solution gel, the core was shut-in for twelve days. After shut-in, water was injected into the core, with an injection corresponding to a pressure gradient of 10 bar/m. The modelled and experimental *RRF* is shown in figure 3-6, where the solid black line is the modelled *RRF* and the blue solid line is the experimental. The *RRF* decreased immediately, which can be explained by that the water injected started to create channels through the gel.

It was found that the RRF depends on the pressure gradient applied on the gel. For a specific silicate concentration, there is maximum pressure gradient that can be applied on the gel, without breaking down the gel. Though, this effect is not investigated in this thesis.

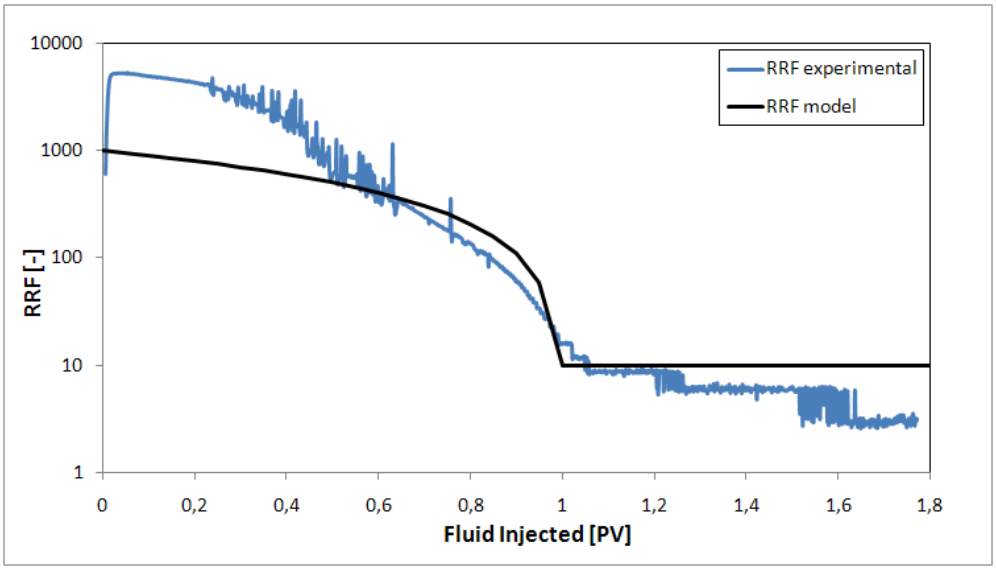

Figure 3-6: Experimental and modelled *RRF*.

4 STARS Simulator Gel Modelling Capabilities

4.1 Introduction

STARS (Steam and Additive Reservoir Simulator) is an advanced process reservoir simulator developed by CMG. The STARS simulator can simulate advanced processes such as chemical/polymer flooding, thermal applications, steam injection, foam and gel treatment (CMG, 2011). The gel modelling in STARS is mainly based on the interaction of chemicals and adsorption/retention of a blocking agent. To form gel, a chemical reaction needs to be defined. When polymer gel is used, the injected fluid has to contain an adsorbing polymer and a non-adsorbing crosslinking agent. After a predetermined time, the polymer and crosslinking agent react and forms a pure blocking gel. The degree of blockage of the pore space, is set by the adsorption data in the model. For a silicate gel the chemical reaction of the model has to contain minimum two components reacting together to form a gel, which is adsorbed/retained to the rock.

STARS contain nine data groups for input of keywords, which have to follow a certain input order in the code. In table 4-1 the most essential keywords for gel modelling in STARS are described. The keyword *MASSBASIS* makes the component property data in the simulator to be based on mass instead of molar mass. The only two exceptions are the definition of molecular weight and the activation energy that have to retain the mole unit. This might be desirable when working with large molecular weights. In this case *MASSBASIS* was used and thereby all of the component property data is based on mass.

4.2 Chemical reaction

4.2.1 Derivation of chemical reaction

Based on the involved chemicals in the experimental data, a simple chemical reaction is derived:

$$sto1_{Si} \cdot Si + sto1_{HCl} \cdot HCl + sto1_{Al3+} \cdot Al^{3+} + sto1_{Ca2+} \cdot Ca^{2+} \rightarrow sto2_{Gel} \cdot Gel \quad (4.1)$$

$sto1_{Si}$: Stoichiometric coefficient of silicate
$sto1_{HCl}$: Stoichiometric coefficient of hydrochloric acid
$sto1_{Al3+}$: Stoichiometric coefficient of aluminium
$sto1_{Ca2+}$: Stoichiometric coefficient of calcium
$sto2_{Gel}$: Stoichiometric coefficient of gel

Table 4-1: Overview of keywords connected to gel modelling in STARS (STARS User's manual, 2009).

DATA GROUP	KEYWORD	PROPERTY
INPUT/OUTPUT CONTROL	MASSBASIS	Component property data is based on mass, i.e. each instance of unit "Molar mass" is interpreted as mass.
	RESTART	Specify time when to restart the simulation.
	WRST	Frequency of writing the restart record.
	FILENAMES	Name of input and output files.
FLUID DEFINITIONS	CMM	Molecular mass of component [kg/gmol].
	STOREAC	Stoichiometric coefficient of reacting component [-]. Enter 0 for non-reacting components
	STOPROD	Stoichiometric coefficient of produced component [-]. Enter 0 for non-produced components in the reaction.
	RPHASE	Set defining phase for reacting component.
	RORDER	Specify order of reaction to each reacting component [-]. Enter 0 for non-reacting components.
	RXCRITCON	Define critical value of reactants concentration factor, below which the dependence of reaction rate on the concentration factor is linear. Use this option when RODER is less than 1.
	FREQFAC	Reaction frequency factor [1/min], which is the same as r_{rk} in equation 2.2
	EACT	Single activation energy gives the dependence of reaction rate on grid block temperature [J/mole]. Reaction rate is independent of temperature when E_a=0.
ROCK-FLUID PROPERTIES	ADSCOMP	Assign name component to which the following adsorption function will apply.
	ADMAXT	Maximum adsorption capacity, which must be positive [kg/(cm^3 PV)]
	ADRT	Residual adsorption level. The allowed range is from 0 to ADMAXT. [kg/(cm^3 PV)]
	RRFT	Residual resistance factor for the adsorbing component [-]. It must be greater or equal to 1.
	ADSTABLE	Denotes that composition dependence is specified via a table of adsorption versus composition.
RECURRENT DATA	INCOMP WATER	Mass fractions of injected water phase [-]. The allowed range for each is 0 to 1.

According to the STARS Users's manual (2009), it is important that stoichiometric coefficients defined for the reacting and produced components are mass conserved, i.e.

$$\sum Mw_i \cdot sto1_i = \sum Mw_i \cdot sto2_i \tag{4.2}$$

M_{wi}: molecular mass of components [kg/gmol]
$sto1_i$: stoichiometric coefficient of reactants [-]
$sto2_i$: stoichiometric coefficient of products [-]

With the given molecular mass of the reacting components in table 4-2, the molecular mass of gel was calculated based on equation 4-2 to be 0,119 kg/gmol.

Based on the equation 4.1, it was initially assumed that the concentration of the injected components was transformed 100% to gel. Thereby, to reflect the injected hydrochloric acid mass, the stoichiometric coefficient of HCl was set to 47,6. For the silicate sodium and aluminium, the relative concentrations of the effluents were known for the dynamic coreflood experiment #3 performed at IRIS. By matching the relative effluent concentrations in figure 3-4 during the experiment, the stoichiometric coefficients for silicate and aluminium were established. The chemical reaction was found to be:

$$47{,}6\ HCl + 0{,}015\ Al^{3+} + 15\ Si \rightarrow 62{,}615\ Gel \tag{4.3}$$

4.2.1 Derivation of reaction rate

The formation of gel is dependent of the kinetic model, also called reaction kinetics. The expression for the kinetic model in STARS is given by equation 2.3.

The concentration C_i for the reacting component is given by:

$$C_i = \phi_f \cdot \rho_j \cdot S_j \cdot w_{ij}, \tag{4.4}$$

where j is the phase which component i is reacting

w_{ji}: mass fraction of component i in phase j [-]
ρ_j: density [kg/cm^3]
S_j: saturation [-]

The reaction rate gives the gel concentration, which is transformed to gel per minute. By replacing the reaction rate by gel concentration divided by gelation time,

$$r_k = \frac{C_{gel}}{t_{gel}} = r_{rk} \cdot e^{-\frac{Ea}{RT}} \cdot \prod_{i=1}^{n_c} C_i^{e_k} \tag{4.5}$$

the gelation time can be calculated for various concentrations of silicate and hydrochloric acid.

$$t_{gel} = C_{gel} \cdot r_{rk}^{-1} \cdot e^{\frac{Ea}{RT}} \cdot \prod_{i=1}^{n_c} C_i^{-e_k} \tag{4.6}$$

As mentioned earlier, the sand column was 100% saturated with water. Thereby, the density ρ_j, would be equal to the water density and the saturation S_j, would equal to 1 for all of the reacting components. The mass fraction is given for each component in table 4-2 from dynamic coreflood experiment 3#. Since calcium is not directly involved in the chemical reaction, the order of reaction is set equal to 0. The activation energy was found to be 77000 J/mole during the bulk experiments. As the experimental gelation times were obtained from the bulk gelation time, the fluid porosity is set equal to 1. The calculated concentrations are shown in table 4-2.

Table 4-2: Overview of mass fractions, concentrations and order of reactions.

Components	**Ca^{2+}**	**HCl**	**Si**	**Al^{3+}**	**H_2O**
Molecular mass [kg/gmol]	4,01E-02	7,29E-02	2,66E-01	2,70E-02	1,80E-02
Mass fraction, w_i [-]	2,00E-05	4,76E-02	4,00E-02	3,10E-05	9,12E-01
Concentration, C_i [kg/cm^3]	2,00E-08	4,76E-05	4,00E-05	3,10E-08	9,12E-04
Order of reaction, e_k [-]	0	3,00	0,10	0,10	0

The frequency factor r_{rk}, and order of reaction e_k, of each reacting component were used as fitting parameters, in order to match the experimental data. With a frequency factor equal to 6,15x10^{19} 1/min, the gelation times are shown at various temperatures in figure 4-1, calculated from STARS. The STARS gelation model matches the derived gelation model in the HCl concentration range 2,5-5%. The experimental data matches the STARS gelation model well for the experiment conducted at the temperature range 40^{o}C - 60^{o}C. At 20^{o}C and 80^{o}C both STARS gelation model and the derived gelation model does not fit the experimental data. To obtain a better match for other HCl concentrations, the frequency factor and order of reactions have to be modified.

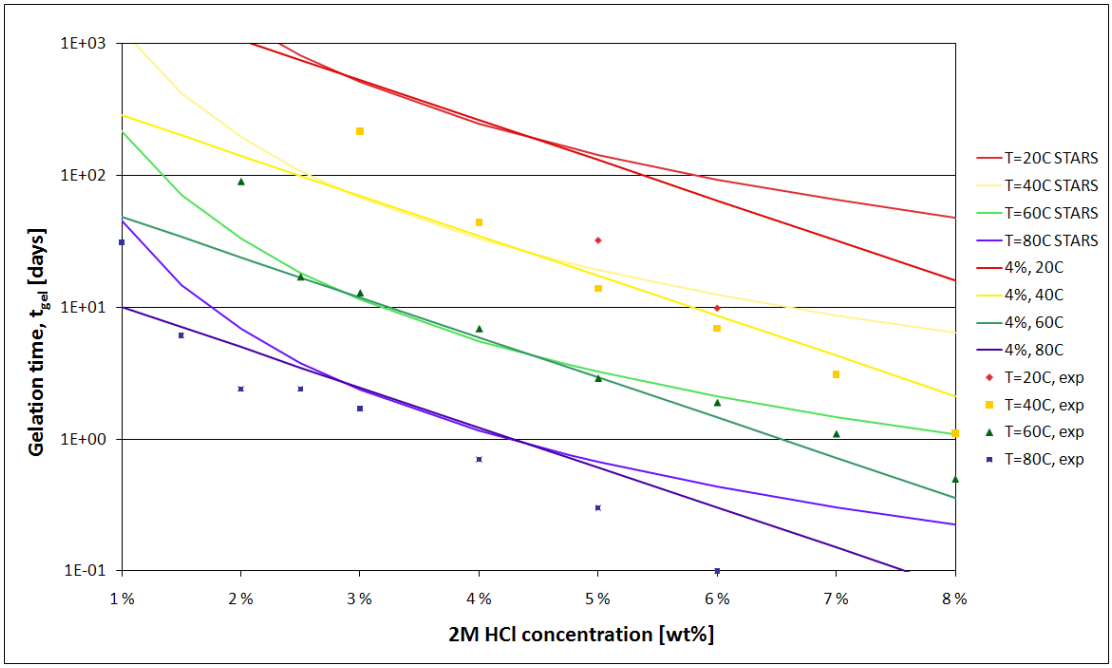

Figure 4-1: Gelation time versus HCl concentration.

4.3 Adsorption/Retention

The blocking mechanism in STARS is based on the adsorption of a defined blocking gel, which is formed by the injected chemicals. By defining gel as an adsorbing component, the gel works as a blocking agent. The adsorption is thereby mechanical. The adsorption can also be reversible, i.e. that the gel does not stick 100% to the rock.

The maximum adsorption level *ADMAXT*, and residual adsorption level *ADRT*, have to be specified, but since the gel adsorption is mechanical, the adsorption is treated as an irreversible process. Therefore, the maximum adsorption is equal to the residual adsorption level. For a reversible process the maximum adsorption is set unequal to the residual adsorption level. The effect of retention is not included in the model, since the gel is defined as an adsorbing agent.

The water phase permeability reduction factor *RKW*, gives the degree of blocking effect. *RKW* is mainly affected by the *RRF* and is defined as:

$$RKW = 1.0 + (RRFT - 1.0)\, AD/ADMAXT \qquad (4.7)$$

RKW: Water phase permeability reduction factor [-]
AD: Variable adsorption level obtained from the concentration [kg/(cm^3·PV)]
ADMAXT: Maximum adsorption capacity [kg/(cm^3·PV)]
RRFT: Residual resistance factor [-]

Beside maximum and residual adsorption levels, the adsorption rate is needed. This can either be done by implementing an adsorption table *ADSTABLE,* in the model, or by the Langmuir parameters A and B (STARS User's manual, 2009). An adsorption table consists of adsorption capacity at a specific gel composition.

4.3.1 Critical concentration and critical gelation time

The gelation kinetics that STARS use is not fully understood. The STARS model creates a significant amount of gel initially. Since gel is defined as the adsorbing component, it will be adsorbed right after it is created. Therefore, the pathways are starting to get blocked at the same time. With a high *RRF*, the *RKW* becomes high. Because of that the differential pressure becomes large. This differs from the theory, where the solution starts to gel at the gelation time, based on the design of the gel. To minimize the blocking effect, the *RRF* is set equal to 1, when the residence time is lower than the gelation time. To obtain blocking at a certain time a restart is done, i.e. the simulation is restarted with a modified *RRF*. Thereby, the *RRF* can be increased to get blocking of the pores.

To deal with this issue the adsorption/retention of the gel is set to start when the gel reaches a specific concentration, which corresponds to the predetermined gelation time. This gel concentration is called the critical gel concentration, which is reached at the critical gelation time. By that means the core reaches its maximum adsorption capacity at the critical gelation time. The maximum adsorption capacity is set equal to the critical gel concentration $C_{cri,gel}$. In that way, the maximum adsorption capacity is reached at critical gelation time $t_{cri,gel}$. By rearranging equation 4.3 the critical gel concentration is given by:

$$C_{cri,gel} = t_{cri,gel} \cdot r_{rk} \cdot e^{-\frac{Ea}{RT}} \cdot \prod_{i=1}^{n_c} C_i^{e_k} \tag{4.8}$$

$C_{cri,gel}$: critical gel concentration [kg/cm^3]
$t_{cri,gel}$: critical gelation time [min]

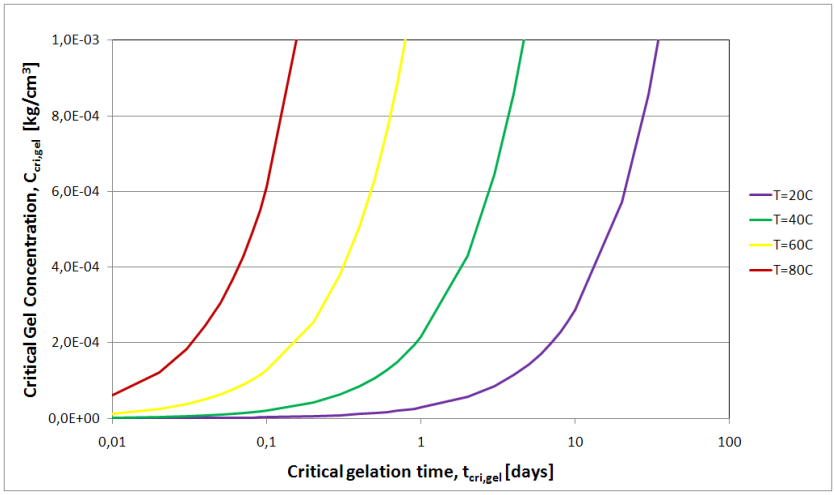

Figure 4-2: Critical gel concentration versus gelation time for dynamic coreflood #3.

Figure 4-2 shows the critical gel concentrations at various gelation times and temperatures for the dynamical coreflood experiment. The gel concentration increases faster with increasing temperature.

4.3.2 Calculation of critical gel concentration

The gel concentration can be calculated based on equation 4.2. It is difficult to calculate the amount of gel net reacted for dynamic corefloods. Since most of the gel is created initially and that not all of the component are 100% transformed to gel. However, the amount of adsorbed gel can be calculated easily by:

$$m_{Gel} = V_{pore} \cdot ADMAXT \qquad (4.9)$$

m_{Gel}: gel mass [kg]

4.3.3 Determine critical gel concentration

The critical gel concentration can be found running the model, without any adsorption data. Thereby, one can observe what the masses of the reacting components are at a specific time, and set the maximum adsorption level to be reached at this time.

With the injection design from the #3 dynamic coreflood experiment, the relative concentrations in figure 4-3 were obtained:

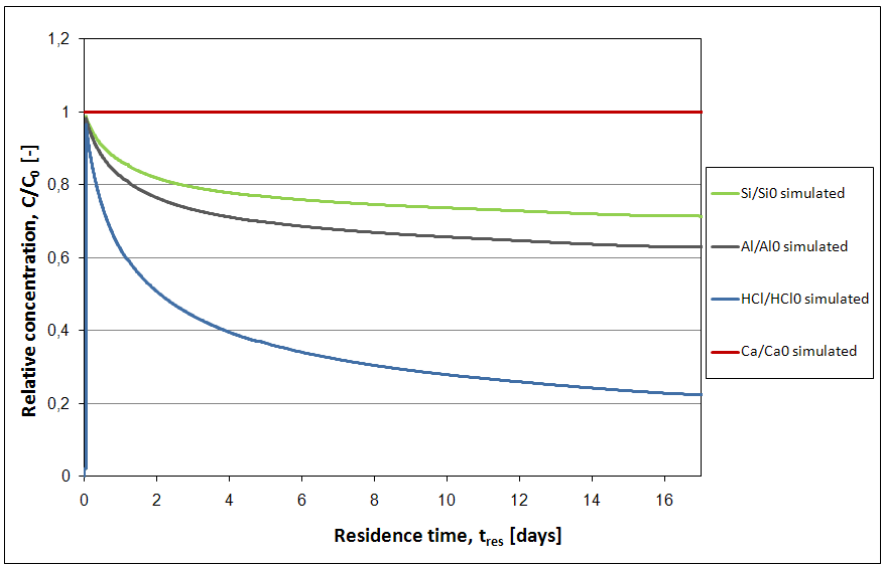

Figure 4-3: Relative effluent concentrations and gel produced obtained from simulation results.

From figure 4-3, the relative concentrations of hydrochloric acid, aluminium and silicate at 13,6 days are 0,25, 0,64 and 0,71. This means that 75% hydrochloric acid, 36% aluminium and 29% silicate have gone into the gel. By multiplying these values with the initial masses of the components and sum them up, a gel mass of approximately 4,8 wt% is obtained. This is about half of what was assumed (cf. 4.2.1).

Since it is uncertain what the gel concentration is at the critical gelation time, the critical gel concentration is set so that *ADMAXT* is obtained over the core at critical gelation time.

4.4 Sensitivity analyses

In order to obtain most accurate data from the simulation, a sensitivity analysis of the number of grid blocks, adsorption data and molecular weight of silicate were done. The sensitivity analysis is based on the dynamic coreflood #3, but certain values differ from the final model used. Because of that, the sensitivity analysis is more to illustrate the effect of adjusting parameters.

4.4.1 Grid block analysis

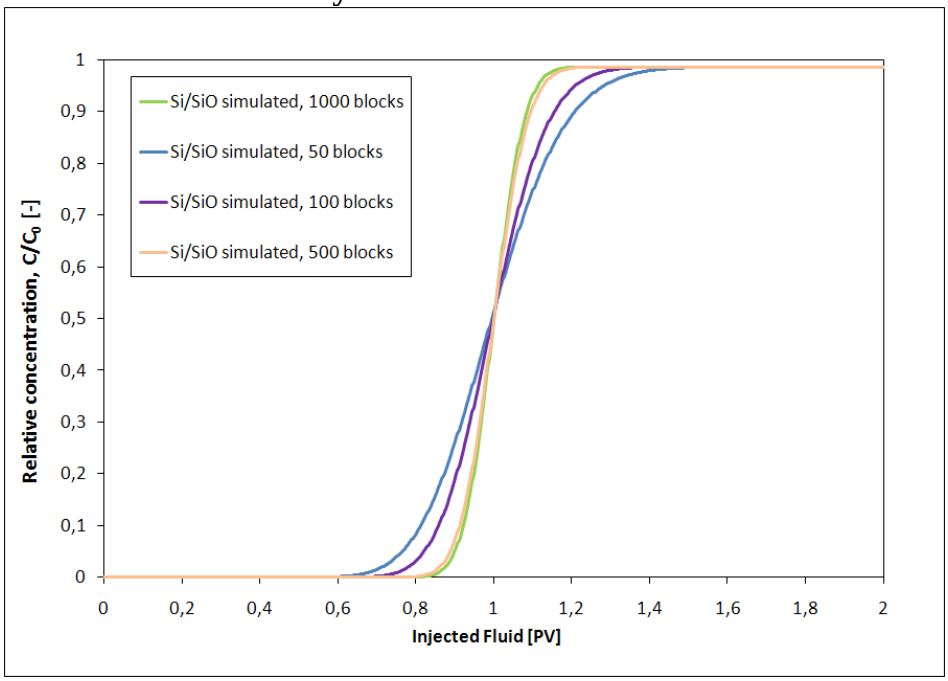

Figure 4-4: Comparison of relative concentrations for various amount of grid blocks.

The size of the grid blocks affects the quality of the results. A sensitivity analysis on different block sizes were run, to determine the effect of number of grid blocks. Figure 4-4 shows that there are significant effect on breakthrough and the relative concentrations of silicate. The case with 10 blocks is starting to get produced at 0,6 pore volumes fluid injected, and the relative concentrations approaches 1 at 1,4 pore volumes fluid injected. The model with 100 blocks starting to get produced at approximately 0,8 pore volumes fluid injected and the relative concentration reaches 1 at 1,3 pore volumes injected. The cases with 500 and 1000 blocks gives more or less the same concentrations and breaks through at producer at the same time.

The effect of grid block size may be explained by the numerical dispersion. While for small grid block sizes there is a sharper shock front, which gives a more realistic result, as the breakthrough of the injected fluids should be close to 1. The disadvantage of the small grid blocks is the increase in simulation time. By increasing the number of grid blocks, the quality of the simulation results would be more accurate, but the disadvantage is that the simulation time increases. To obtain a more accurate result, the amount and size of timesteps can be increased, which is frequency of outputting values in the simulation.

4.4.2 Adsorption data analysis

The *RRF* plays an important role regarding the adsorption and the blocking effect of the gel treatment, since the *RRF* significantly affects the *RKW*. In the case shown in figure 4-5, the core has adsorbed a certain amount of gel. The case is run with different *RRF* values, to study the effect of *RRF*, connected with the differential pressure. With a RRF equal to 1, the differential pressure does not change at all. At a *RRF* equal to 7500 the differential pressure increases to 750 mbar. It seems that the differential pressure increases by approximately 400 mbar by increasing the *RRF* by 2500.

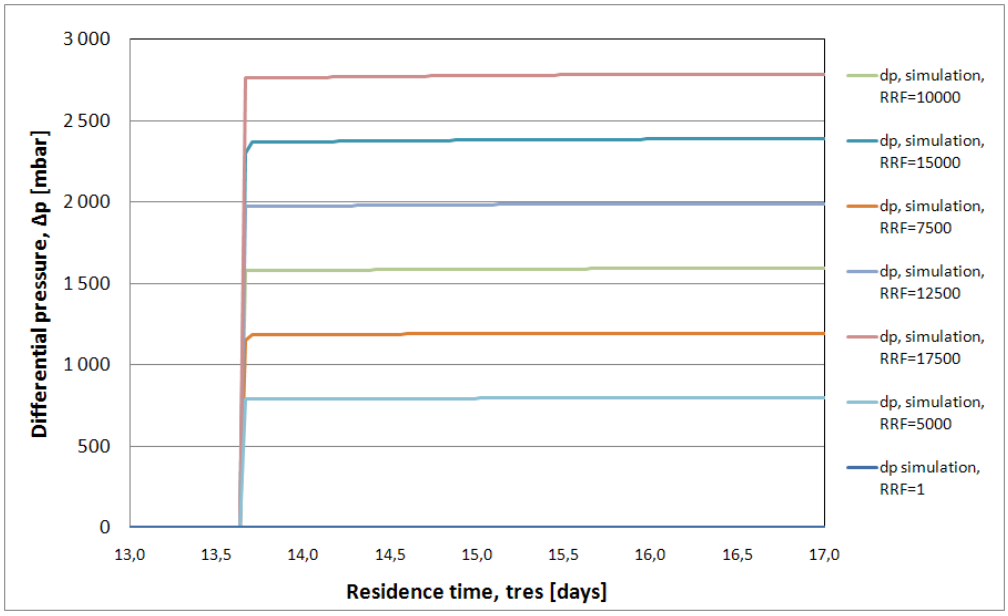

Figure 4-5: Comparison of differential pressures with different *RRF*.

The reversible adsorption was also analyzed to study the effect of *ADRT*. Four different cases were run in the post shut-in period with water. After a shut-in period of 12 days, water was injected with a rate of 0,05 ml/min. By injecting water, gel is desorbed from the core, until ADRT is reached. The first one was with *ADRT* equal 100% *ADMAXT*, which is shown with the blue curve in figure 4-6. This is the same as irreversible adsorption. The red curve with *ADRT* equals to 50% of *ADMAXT*. The third case was with ADRT equal to 10% of *ADMAXT*, which is shown by the green curve. The purple curve was with *ADRT* equals to 0 % of *ADMAXT*.

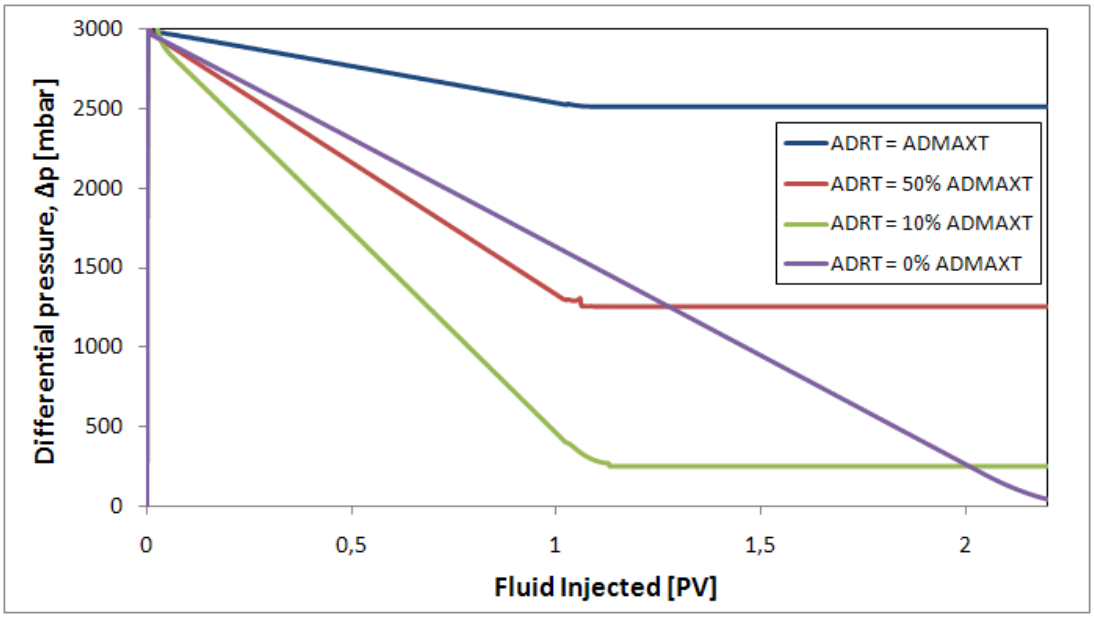

Figure 4-6: Comparison of differential pressure with different *ADRT*.

From figure 4-6 it seems that the all of the cases except the one with *ADRT* equals to 0 gets a stable differential pressure at 1 pore volume water injected. The case with *ADRT* equals to 0 obtain a stable differential pressure at 2,2 pore volumes water injected, which is about 0 mbar.

4.4.3 Molecular weight analysis

According to equation 4.2 the mass of the reactants and products should be balanced. Therefore, by changing the molecular weight of silicate, the molecular weight of gel would be affected. The molecular weight of $(SiO_2)_{3,4}$:Na_2O, is 0,2663 kg/gmol. By decreasing the silicate molecular to 0,06 kg/gmol, which is the molecular weight of SiO_2, the molecular weight of gel decreases to 0,0701 kg/mol. Figure 4-7 shows the gel reacted, produced and adsorbed of the cases with molecular weight of silicate equal to 0,2663 kg/mol and 0,06 kg/mol. The produced and reacted gel is approximately the same for each case, but there is a significant effect on the amount of gel adsorbed.

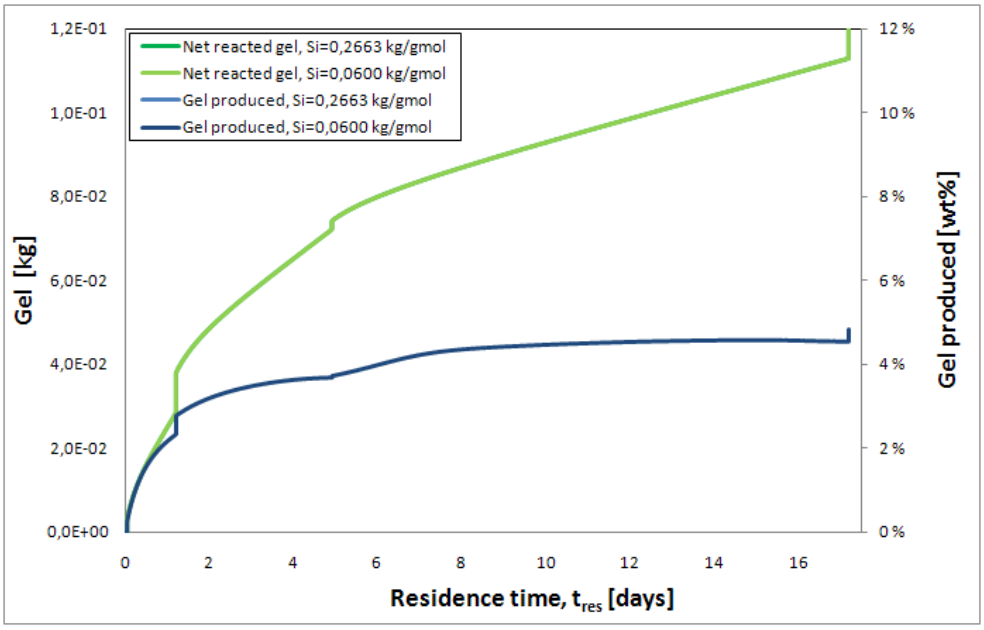

Figure 4-7: Comparison of different silicate molecular weight.

On figure 4-8 it can be seen that the amount of gel adsorbed increases from around $4{,}0 \cdot 10^{-3}$ kg to $6{,}0 \cdot 10^{-3}$ kg. The main reason for the increasing amount of adsorbed gel is that the maximum adsorption level is set to gel concentrations, corresponding to the molecular weight of gel. Since the molecular weight of gel decreases, it takes less time for the gel to get formed. Also, the maximum adsorption capacity of gel also decreases. In that way, more gel will be adsorbed to the core, compared to the case with molecular silicate weight of 0,06 kg/gmol.

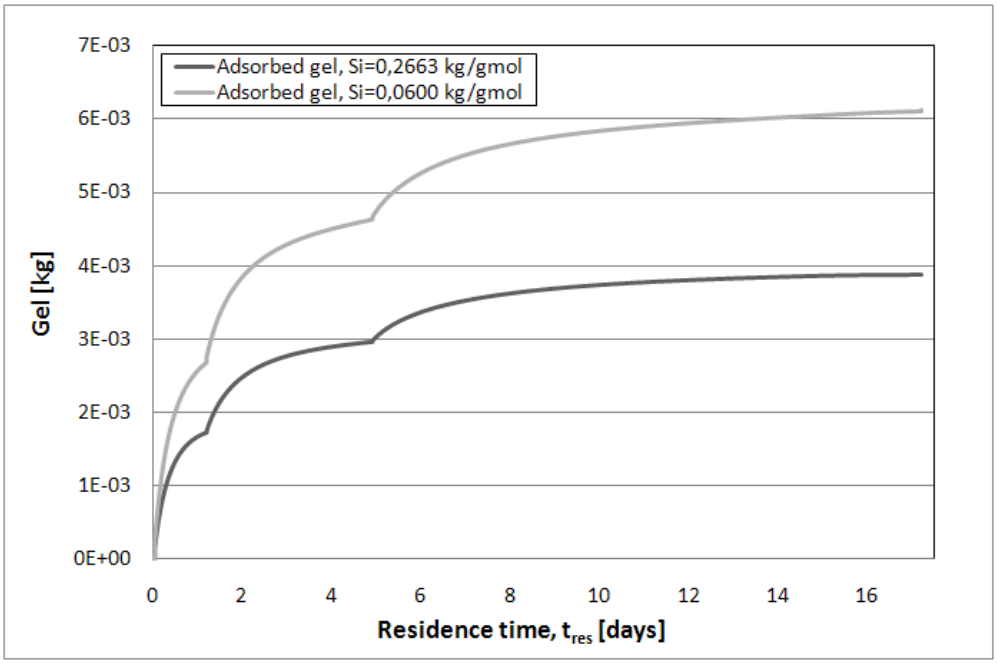

Figure 4-8: Gel adsorption with different adsorption data.

5 Simulation Models

Based on the sensitivity analysis in (cf. 4.4), it was decided to use 1000 grid blocks for the models, and use the molecular weight of $(SiO_2)_{3,4}$:Na_2O, which was 0,2662 kg/gmol. To obtain the blocking effect at the plugging/gelation time, the RRF was modified to 8000 at this point for the dynamic coreflood experiment. Otherwise, the *RRF* was set equal to 1.

5.1 Dynamic coreflood experiment

5.1.1 Reservoir description

Experiment #3 of the dynamic flood experiment consisted only of one sand column, with a length of 75 cm. The permeability of the sand column was set to be 41% and 9000 mD. The core diameter was 5,36 cm. However, due to difficulties with modelling a core with rounded cross-sectional area, the model contained a squared cross-sectional area instead. The diameter used in the model was thereby 4,75 cm in order to obtain the same cross-sectional are as the core.

Table 5-1: Reservoir description in dynamic coreflood experiment #3.

Grids [x,y,z]	1000,1,1
Core length [cm]	75,00
Core diameter [cm]	4,75
Porosity [-]	0,41
Permeability, i [mD]	9000
Permeability, k = i = j	
Pore volume [ml]	700

5.1.2 Chemical reaction

An overview of the calculated concentrations and order of reaction used for the injected components, are shown in table 5-2. The reacting components had an order of reaction unequal to 0. The temperature in the experiment was 55^{o}C. To get a gelation time of 13,6 days, the reaction constant was set to $6{,}15 \times 10^{19}$ 1/min (cf. Appendix 4). The fluid porosity used was 0,41. The match of gelation time for various HCl concentrations can be seen in figure 4-1.

Table 5-2: Overview of mass fractions, concentrations and order of reactions from dynamic coreflood #3.

Components	**Ca^{2+}**	**HCl**	**Si**	**Al^{3+}**	**H_2O**
Molecular mass [kg/gmol]	4,01E-02	7,29E-02	2,66E-01	2,70E-02	1,80E-02
Mass fraction, w_i [-]	2,00E-05	4,76E-02	4,00E-02	3,10E-05	9,12E-01
Concentration, C_i [kg/cm^3]	8,20E-09	1,95E-05	1,64E-05	1,27E-08	3,74E-04
Order of reaction, e_k [-]	0	3,00	0,10	0,10	0

5.1.3 Permeability data

The experiment consisted of a single phase flow, and the permeability data were modified accordingly, in order to reduce the effect of relative permeability of oil and gas.

5.1.4 Adsorption data

Based on figure 4-3 the gel mass in the core was found at 13,6 days to be 4,8 wt%. Thereby, the model is set to reach *ADMAXT* at this gel composition. Since the adsorption is irreversible, the maximum adsorption capacity is set equal to the residual adsorption level. In this case the adsorption is set to $2{,}0 \cdot 10^{-5}$ kg/(cm^3 PV), to reach *ADMAXT*. The *RRF* was set to 8000 at 13,6 days, to match the differential pressure from figure 3-3.

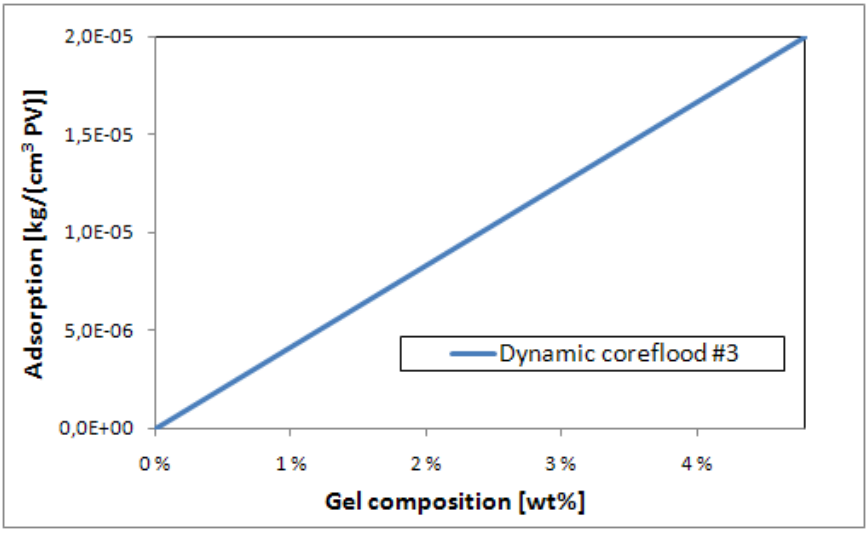

Figure 5-1: Adsorption versus gel composition in the core for the dynamic coreflood.

5.1.5 Injection design

The composition of the injected fluid is given by the mass fraction in table 5-2. During the dynamic coreflood experiment, the injection rate varied from 0,03 ml/min to 11,7 ml/min. Since the gelation time was set to 13,6 days, the residence time would not be sufficient enough for the injection rates lower than 0,03 ml/min. An overview of the injection rates obtained at various times can be seen in figure 3-3.

5.2 Static coreflood experiment

The main object of the static coreflood experiment was to study the gel strength of the silicate gel. The experiment was divided into three phases; injection of silicate, shut-in period and post shut-in period.

Initially five pore volumes of silicate solution were injected into the sand column, and then shut-in for twelve days. After the shut-in period water was injected.

5.2.1 Reservoir description

The sand column used for the shut-in case was 30,3 cm long, and had a pore volume close to 80 ml. The porosity of the sand column was given to be 26%. Based on that information, the core diameter was calculated to be 3,19 cm. Also in this case, 1000 grid blocks were used.

Table 5-3: Reservoir description in static coreflood experiment.

Grids [x,y,z]	1000,1,1
Core length [cm]	30,30
Core diameter [cm]	3,19
Porosity [-]	0,26
Permeability, i [mD]	8000
Permeability, k = i = j	
Pore volume [ml]	80

5.2.2 Chemical reaction

With the concentration in table 5-4, the gelation time was calculated to 1,7 days. As the gelation time is higher than the residence time of the injected fluid, gel would not be created after the well is shut-in. An overview of the calculated concentrations and order of reaction used, are shown in table 5-4. The temperature in the experiment was 40^{o}C and the fluid porosity used was 0,26. The match of gelation time from the STARS model and experimental data, for various HCl concentrations can be seen in figure 5-2. The frequency factor was equal to 1,85x10^{25} 1/min. There is a good match with the experimental data for HCl concentration above 7 wt%.

Table 5-4: Overview of mass fractions, concentrations and order of reactions from static coreflood.

Components	**Ca^{2+}**	**HCl**	**Si**	**Al^{3+}**	**H_2O**
Molecular mass [kg/gmol]	4,01E-02	7,29E-02	2,66E-01	2,70E-02	1,80E-02
Mass fraction, w_i [-]	2,00E-05	8,50E-02	3,00E-02	3,10E-05	8,85E-01
Concentration, C_i [kg/cm^3]	5,20E-09	2,21E-05	7,80E-06	8,06E-09	2,30E-04
Order of reaction, e_k [-]	0	4,00	0,10	0,10	0

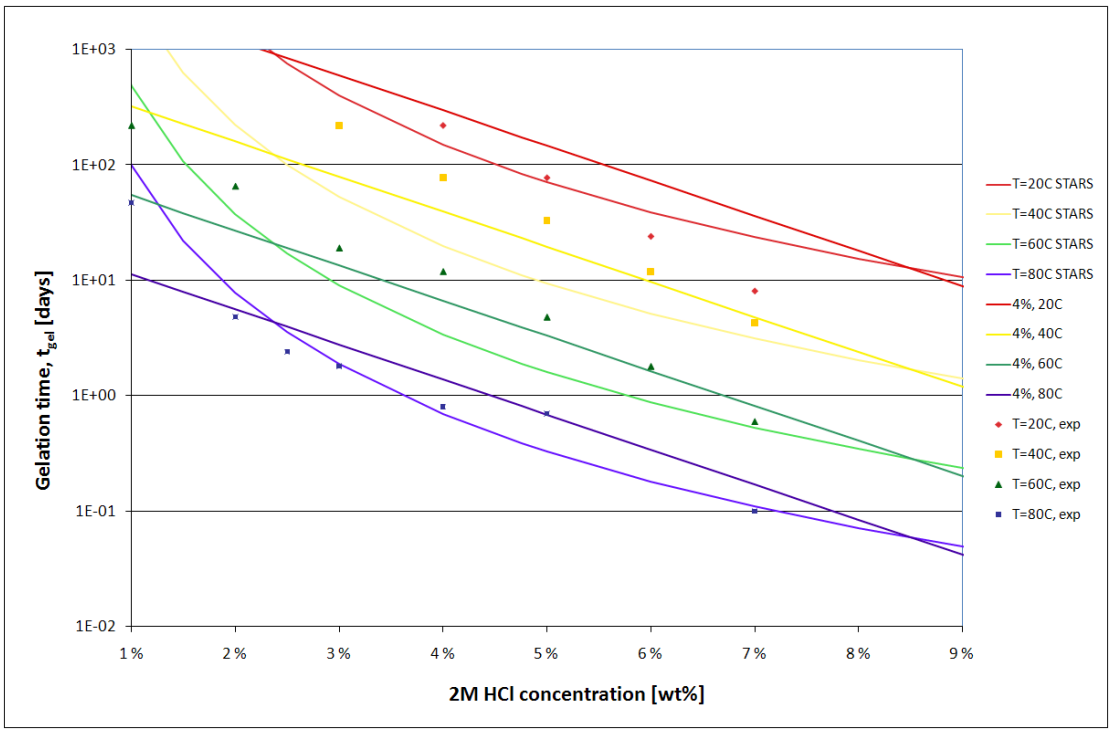

Figure 5-2: Matching the experimental and STARS gelation time for the injection design in the static coreflood experiment.

5.2.3 Permeability data

Since this experiment also consisted of studying a single phase flow, the permeability data were modified accordingly, as in the dynamic coreflood experiment.

5.2.4 Adsorption data

With the injection design given in table 3-4 gelation time was calculated to be approximately 1,7 days, when the gel content in the core was 4,8 wt%. In this case the adsorption is set equal to $1{,}0 \cdot 10^{-6}$, in order to get 100% adsorption of gel at the critical gelation time. To match the *RRF* in the post shut-in period, the *RRF* was set equal to the experimental *RRF*, which is shown in figure 3-4. For each 0,1 pore volume fluid injected, the simulation was restarted with a modified *RRF*, in order to match the experimental *RRF*. For $5000 < RRF < 20$, irreversible adsorption was used to match the experimental differential pressure. Outside this range reversible adsorption was used.

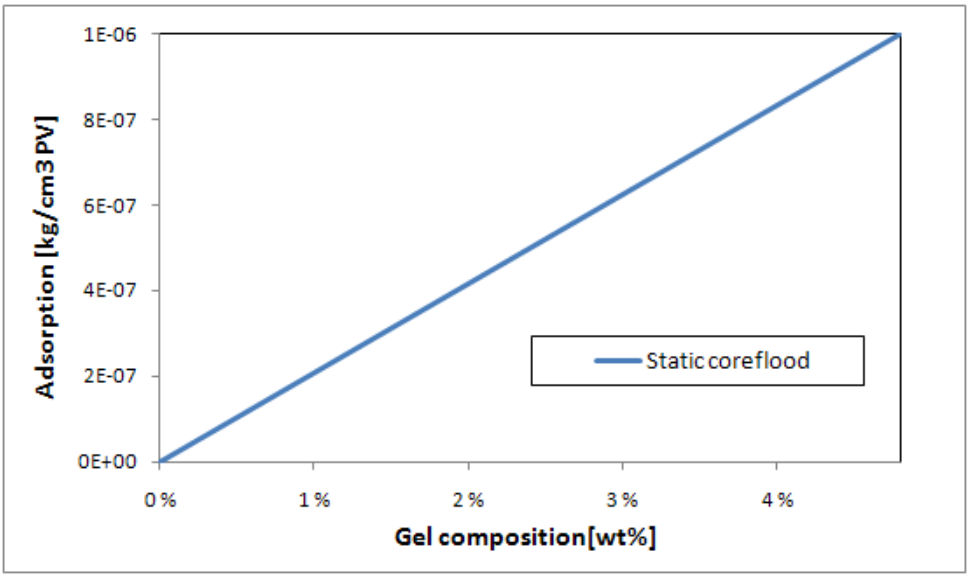

Figure 5-3: Adsorption versus gel composition for the static coreflood.

5.2.5 Injection design

The injection rate was 5 ml/min for the first period, and then 0,05 ml/min for the post shut-in period. The well was shut-in after 80 min. After approximately 12 days water was injected until a stable *RRF* was reached.

6 Results and Discussion

Two cases were modelled and history matched with the experimental data; the static coreflood experiment, and #3 of the dynamic coreflood experiments. In the dynamic coreflood experiment, focus was put on history matching the differential pressure, injection rate and the effluent relative concentration (cf. 3.2). For the static coreflood experiment the focus was put on history matching the *RF* in the injection of silicate solution period, and the *RRF* in the post shut-in period (cf. 3.3).

6.1 Dynamic coreflood experiment

6.1.1 Matching of relative concentrations of effluents

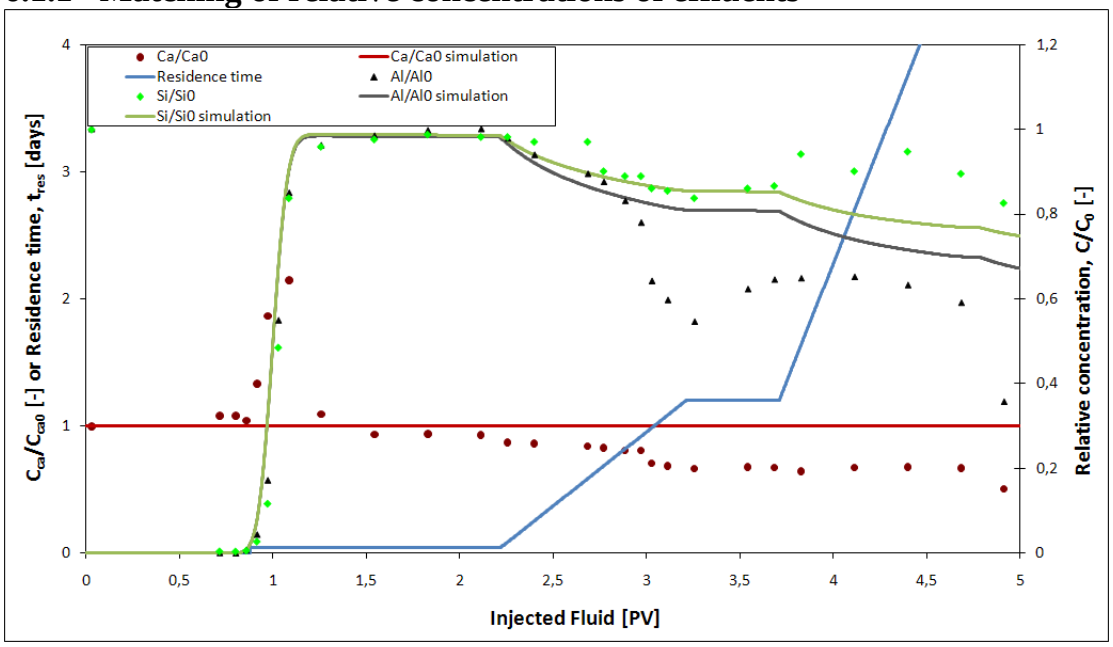

Figure 6-1: Effluent concentration versus PV, experimental and simulation.

The relative concentrations of effluents are plotted versus fluid injected in the core in figure 6-1. The rounded brown dots are the relative concentration of calcium from the experiment, the green squared dots are the relative silicate concentration from the experiment, and the triangular black dots are the relative aluminium concentrations obtained from the experiment. The solid light brown line is the relative calcium concentration obtained from the simulation. The solid green and grey line is the relative silicate and aluminium concentration obtained from the simulation results. The solid blue line is the residence time connected to the injected fluid.

Only the concentrations during the first three injection rates are sampled during the experiments, due to plugging of the back regulator. At 1 pore volume fluid injected there is a significant increase in relative concentration of all of the components, due to the breakthrough of the injected fluid. After breakthrough and the whole period with injection rate equal to 11,7 ml/min, the concentration of silicate and aluminium were

close to 1. This is a result of the low residence time, linked with the high injection rate. The residence time is lower than the predetermined gelation time, which was 13,6 days. Because of that no gel will form. Visualization of the core can be seen in figure 6-2, which shows that no gel is adsorbed in the core. The amount of gel adsorbed is shown by the colour in the core, which is described on the scale to the right. Colour red represents the maximum adsorption level. The relative concentration of silicate, calcium and aluminium obtained from the simulation matches well with the experimental data for the first injection rate.

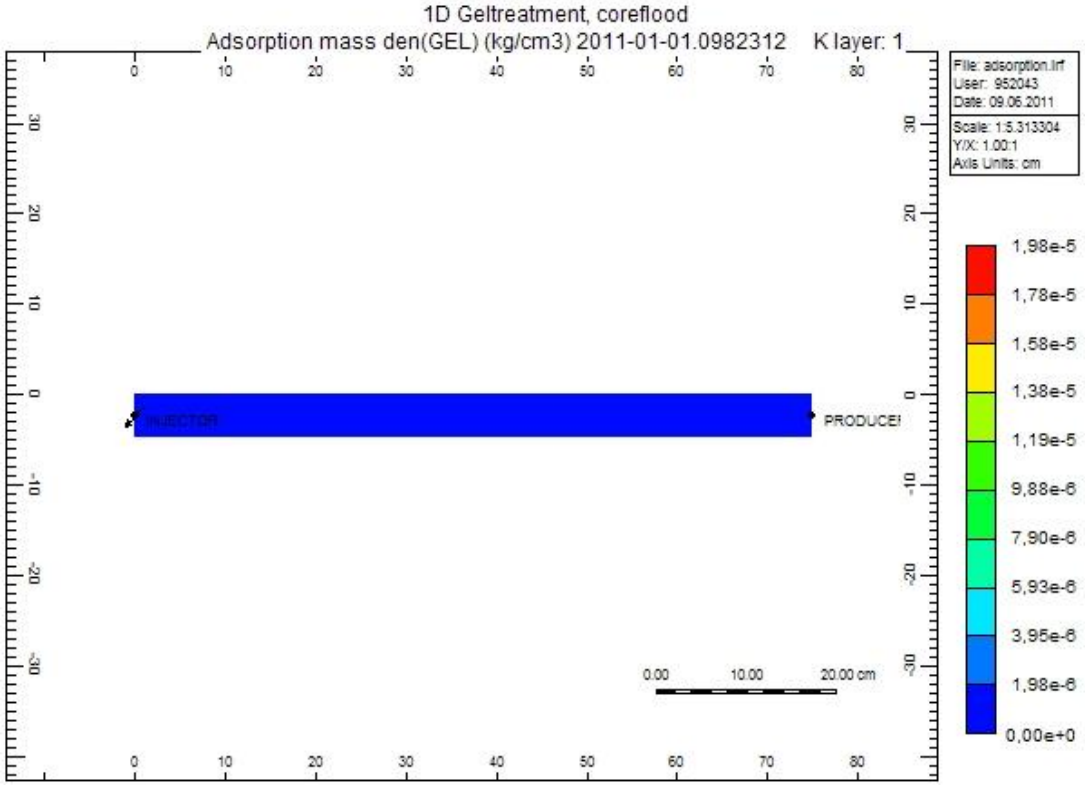

Figure 6-2: Adsorbed gel at the end of first injection period.

After 2,2 pore volumes fluid injected, the injection rate decreases to 0,4 ml/min. At the same time, the relative concentration of both aluminium and silicate starts to decrease. This means that silicate and aluminium is starting to react and go into the gel structure. At 2,7 pore volumes fluid injected, the relative aluminium concentration from the experimental data rapidly increases, while the relative concentration of silicate decreases slower. The relative concentration from the simulation matches well with the behaviour of the silicate, and partly the relative concentration of aluminium for this period. To obtain a better match the behaviour of aluminium, the order of reaction for aluminium can be increased. Thereby, more of the aluminium will react in the model, and the relative concentration of aluminium will decrease faster at this point. Figure 6-3, shows the adsorbed gel content in the core after 3,7 pore volumes injected. Most of the gel has been adsorbed in the end of the core, and the mass of adsorbed gel decreases towards the inlet of the core. Since the residence time is higher for the fluid in the end, compared to the inlet, more gel has been created and been adsorbed in this part of the core.

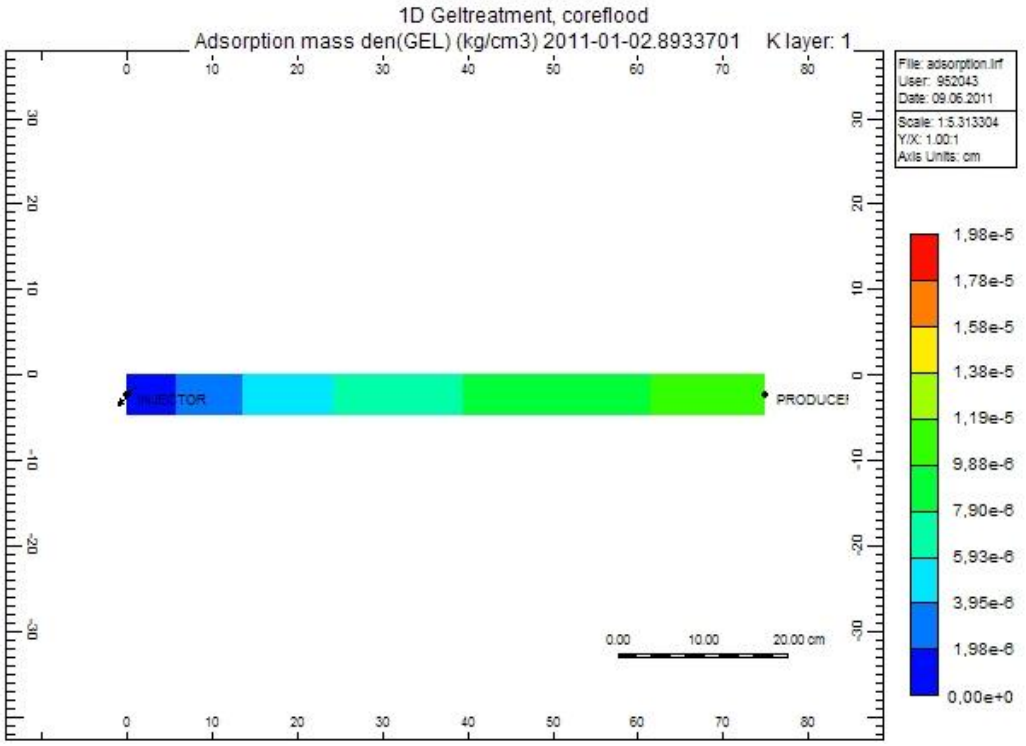

Figure 6-3: Adsorbed gel at the end of the second injection period.

At injection rate equal to 0,098 ml/min, which corresponds to 3,7 pore volumes fluid injected, the concentrations of both silicate and aluminium start to increase again in the experimental data. It is not completely understood why the concentrations starts to increase again. At 4,7 pore volumes fluid injected the injection rate decreases to 0,028 ml/min, and the relative concentrations of all of the components decreases again, which can be seen in figure 6-1.

After 5 pore volumes fluid injected the filter was plugged, and the relative concentrations were not sampled after that. As the residence time increases with decreasing injection rate, the gel formation increases. Thereby, the concentration of both aluminium and silicate decreases with the same trend as the gel is formed, which can be seen in figure 4-3. The visualization of the gel content in the core is shown in figure 6-4, at 5 pore volumes fluid injected. Compared to figure 6-3, more gel has been adsorbed in the same pore space as the previous adsorbed gel.

The relative concentration of calcium is equal to 1 during the whole run, since it is not part of the reaction in the simulation model. The calcium concentration from the simulation results, matches the experiment well until 2,2 pore volumes fluid injected. Figure 6-2 shows that no gel has been adsorbed at this time. Thereby, the relative calcium concentration would not be reduced. Seen from the experimental data, the calcium content affects the gelation process. In table 3-2 the gelation time increases by increasing calcium content in the silicate solution. As the calcium is not part of the chemical reaction, it is difficult to catch the calcium behaviour in STARS. By including it in the chemical reaction, it can be possible to model the calcium performance.

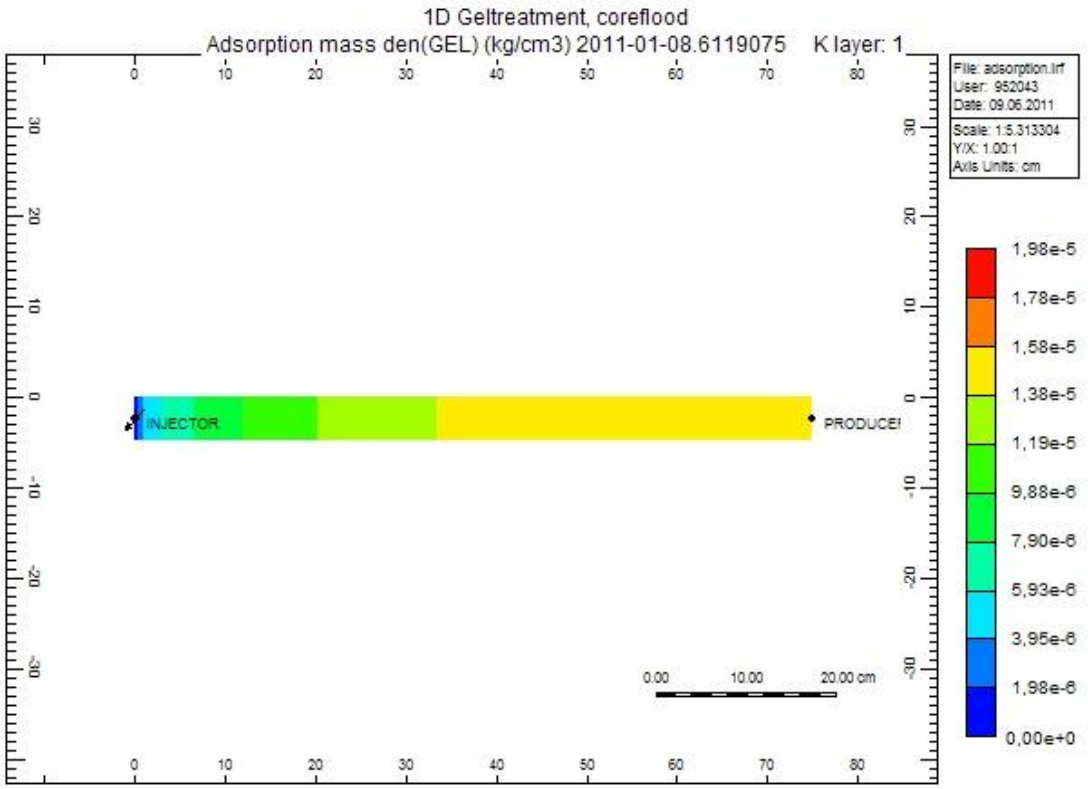

Figure 6-4: Adsorbed gel at the end of the third injection period.

Overall, the simulation output matches the experimental data well at the first rate. At the second injection rate and when gel is starting to get formed, the relative concentration of all the components starts to decrease as a result of the reaction of the gel formation. Only the relative concentration of silicate is matched at this stage. It is possible to get a better match of the aluminium concentration by increasing the order of reaction of these components, to make more of the aluminium to react. Calcium is not a part of the chemical reaction, but seen in the experimental data, it affects the gelation time. It can be possible to catch the behaviour of the calcium by implementing it in the chemical reaction.

6.1.2 Matching of differential pressure and liquid rate

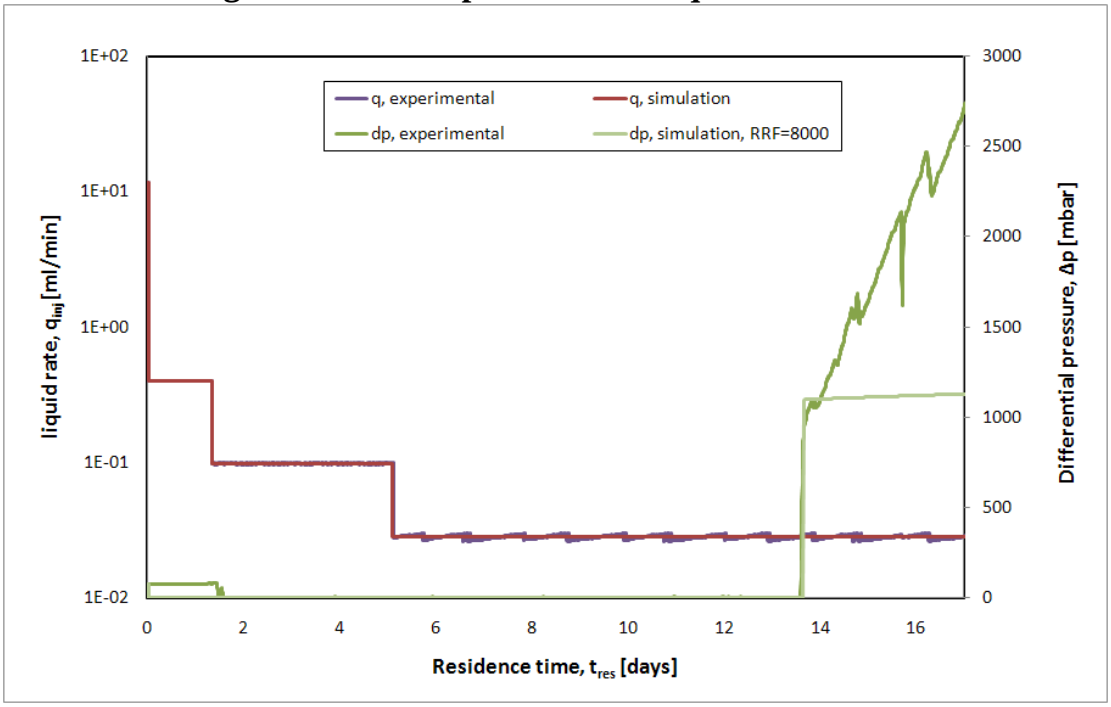

Figure 6-5: Differential pressure and injected rate versus time, experimental and simulation.

The differential pressure and the injection rate are plotted versus the residence time in figure 6-5. The red solid line is the simulated injection rate, and solid purple line is the injection rate obtained from the experimental data. The solid green line is the differential pressure from the experiment, the lighter green solid line is the differential pressure obtained from the simulation results. In order to match the differential pressure the *RRF*'s has to be modified at the plugging time.

For injection rate equal to 11,7 ml/min the residence time is small, i.e. too little in order to form gel in the core. Figure 6-1 shows that the relative concentrations of both silicate and aluminium are approximately 1 in this period. Visualization of gel in the core can be seen in figure 6-2, which shows no gel at the end of the first injection period. In the experimental data there is a minor pressure increase during the first two injection rates. From approximately 0,01 days to 1,5 days, the injection rate 0,04 ml/min is applied. This rate also gives a too short residence time in order to form gel in the core. In figure 6-1 the relative concentrations starts to decrease at this point, which means that gel has started to create. Figure 6-3 shows that gel has started to get adsorbed in the end of the core at this point.

The residence time corresponding to the injection rate of 0,098 ml/min is also too small, in order to get sufficient gel size to plug the core. Figure 6-4 shows that more gel has been attached to the core obtained from the simulation results, especially in the end of the core.

For the last injection rate of 0,028 ml/min the residence time is sufficient enough to plug the core. At a residence time equal to 13,6 days the differential pressure from the experimental data increases to approximately 1000 mbar, which means that the core is starting to get plugged. After 13,6 days the differential pressure from the experimental data increases further until it reaches 2700 mbar, and at 17 days the core was completely plugged. Figure 6-5 shows the differential pressure *RRF* equal to 8000, but since the injection rate is quite low during this period, the experimental data after 13,6 days is not very reliable (Stavland, 2011). Figure 6-5 shows a good match of the differential pressure at 13,6 days. The *RRF* at this stage is 8000. To catch the behaviour of the differential pressure, the *RRF* in the adsorption data has to be increased in order to create the blocking effect.

In the simulation the differential pressure follows mostly the trend of the injection rate. This can be seen in figure 6-5. At high injection rates, there is a increase in differential pressure. In order to match the differential pressure from the experimental data, the *RRF* in the adsorption data is modified. By increasing the *RRF* at the designed gelation time, the preferable differential pressure can be obtained. At 13,6 days the *RRF* is set to 8000, to match the experimental data. In the experiment data the pressure increased rapid to 1000 mbar at 13,6 days, and increased further to 2700 mbar. Visualization of the gel adsorbed in the core at 13,6 days is shown in figure 6-6. A large amount of the core has reached the maximum adsorption capacity

.

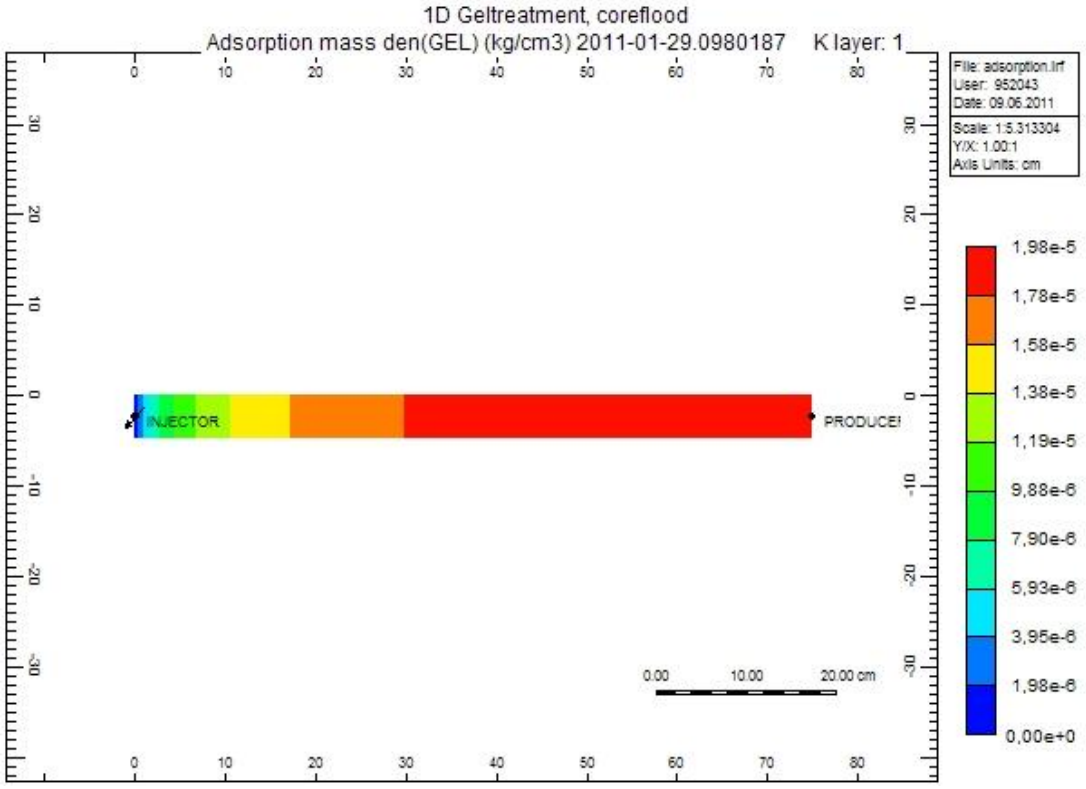

Figure 6-6: Adsorbed gel at residence time = 13,6 days.

6.1.3 Amount of gel reacted and adsorbed/retained

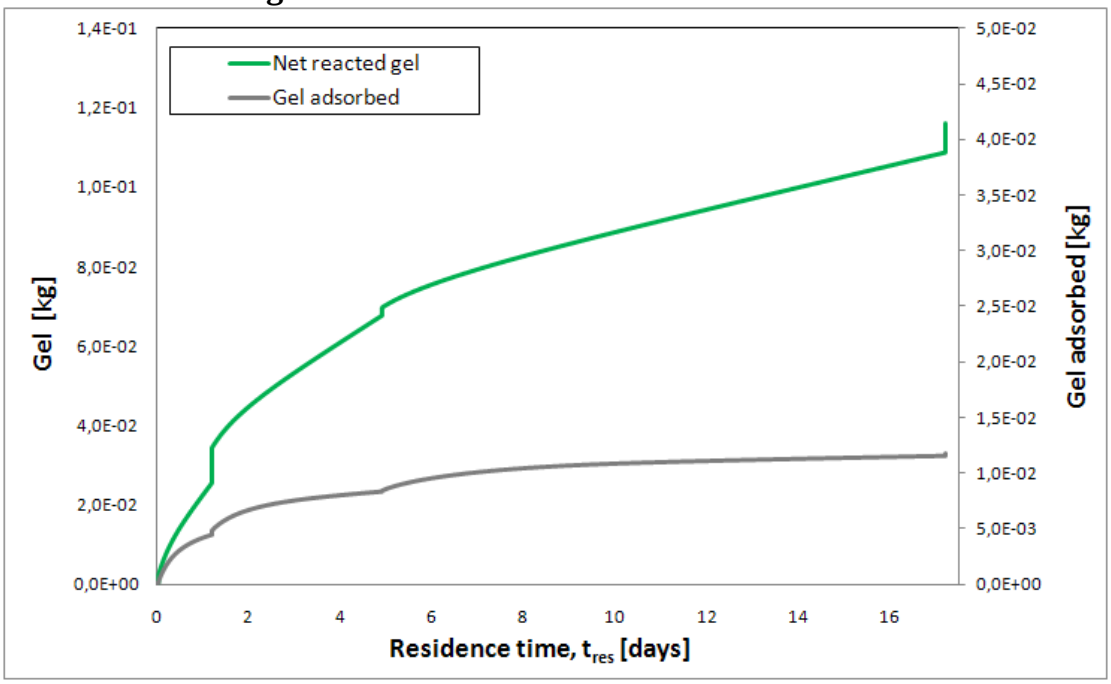

Figure 6-7: Gel reacted and gel adsorbed/retained versus residence time.

Figure 6-7 shows the amount of gel net reacted and gel that has been adsorbed, where the green solid line shows the net reacted gel and the grey solid line shows the gel adsorbed. According to figure 6-7 gel is formed continuously and most of the gel is formed in the start. The slope of gel created decreases with time.

By taking the net reacted gel mass at the end of each period with different injection rate, it is possible to calculate a general reaction rate connected to each injection rate, based on equation 4.2 (cf. Appendix 3). At a residence time of 0,04 days, $2{,}65 \cdot 10^{-3}$ kg gel is created. By that time 2,2 pore volumes has been created, which gives a reaction rate of $1{,}31 \cdot 10^{-8}$ kg/(min·cm^3). From 0,04 days to 1,2 days, $3{,}18 \cdot 10^{-2}$ kg gel has been created and 1,5 pore volumes has been injected. This gives a reaction rate of $1{,}17 \cdot 10^{-8}$ kg/(min·cm^3). At 1,2 to 5 days $3{,}26 \cdot 10^{-2}$ kg has been transformed into gel, at the same time as approximately 1,1 pore volumes has been injected. This gives an reaction rate of $5{,}91 \cdot 10^{-9}$ kg/(min·cm^3). In the last period $4{,}63 \cdot 10^{-2}$ kg gel has been created, while 1,2 pore volumes has been injected. This gives a reaction rate of $3{,}12 \cdot 10^{-9}$ kg/(min·cm^3). The slope of the net reacted is affected by the injection rate, which can be seen on the increasing reaction rate connected to each injection rate.

The majority of the gel is adsorbed initial, until the gel content in the core reaches its maximum adsorption capacity. At 13,6 days the slope of the adsorbed gel curve start to slow down. This mainly because the adsorption data is set to maximal adsorption level at this time, which corresponds to a predetermined gel concentration and gelation time.

As a result that the gel is formed continuously, the gel is also adsorbed continuously. Thereby, the core would be plugged in the beginning, and the pressure would also increase. It is difficult to calculate the net reacted in this case, because most of the gel is created in the start. Connected to figure 4-3, not 100% of the injected components are transformed into gel. By multiplying the relative concentration of each reacting component, the gel concentration can be found at a specific time step. With the relative concentrations at 17 days in figure 4-3 the gel concentration at 17 days was calculated to be $3{,}32 \cdot 10^{-4}$ kg/cm^3 (cf. Appendix 1) The total injected volume was 6 pore volumes, which gives a gel mass of 0,14 kg. The net reacted gel obtained from the simulation results was 0,12 kg. The mass gel from the simulation results is lower than the calculated, but by integrating the relative concentrations throughout the simulation, a more accurate gel mass can be found. With the calculated gel concentration, this corresponds to a volume of 672 ml, given that 100% of the reactants are transformed to gel.

The adsorbed gel mass from the simulation was $1{,}19 \cdot 10^{-2}$ kg and the calculated adsorbed gel mass was $1{,}50 \cdot 10^{-2}$ kg, based on equation 4.9 (cf. Appendix 1). Figure 6-6 shows that not the whole core has reached the maximum adsorption capacity. Thereby, the calculated adsorbed gel should be a bit lower.

Overall, it is difficult to calculate the net reacted gel connected to dynamic flooding, but the calculations for adsorbed gel mass matches the gel mass from the simulation results.

6.2 Static flooding experiment

6.2.1 Injection of silicate solution – matching of *RF*

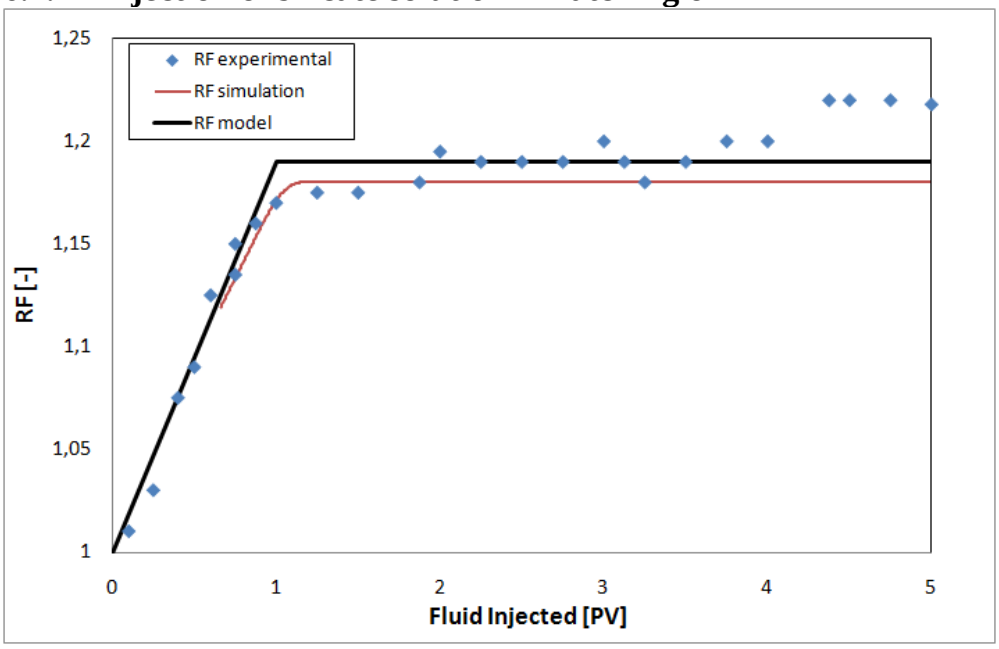

Figure 6-8: *RF* versus fluid injected.

The black solid line in figure 6-8 is the modelled *RF*, the red solid line is the *RF* obtained from the simulation, and the blue dots are the experimental data. The RF's in all methods start at 1 and increases until 1 pore volume fluid is injected. After that the whole core is filled with silicate solution, and the *RF* would be constant the rest of the injection period. While the modelled *RF* reaches a value of 1,19 the simulated *RF* is 1,17, which gives a good match with the experimental data until around 2 pore volumes fluid injected. At 2 pore volumes fluid injected, the experimental *RF* increases to 1,19 and further to 1,23 at 4,3 pore volumes fluid injected. This can be explained by that gel aggregates are starting to getting formed, and increasing the viscosity of the fluid, which mainly affects the *RF* at this stage. It would be possible to match the *RF* after 2 pore volumes fluid injected, but it is difficult to foresee when gel aggregates are formed.

Based on equation 3.1, the gelation time of the injected fluid was calculated to be approximately 1,7 days. By that means no gel would be formed during this injection period, which is about 18 minutes. The permeability does not alter, but the viscosity of the water is affected by the injected fluid, and thereby the *RF* increases to 1,2. Figure 6-9 shows the gel content in the period after the injection, and some gel has been adsorbed in the core, especially in the end of the core.

Generally, the *RF* is mainly affected by the viscosity of the silicate solution when the residence time is lower than the designed gelation time. The simulation results correspond well with the experimental data.

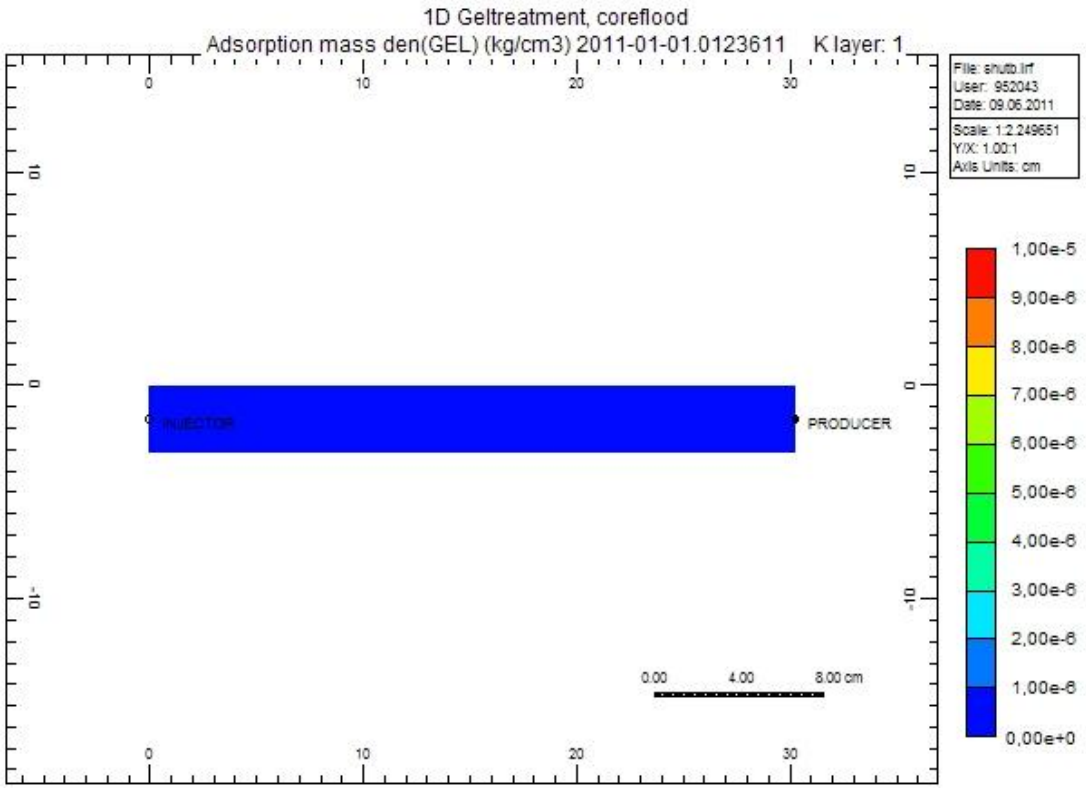

Figure 6-9: Gel in the core after the injection of silicate solution.

6.2.2 Shut-in period – amount of gel created

After the injection period the core was shut-in for 12 days, so that gel would grow. In figure 6-10 the net reacted gel is shown in the red solid line and the gel adsorbed in blue solid line. The adsorption curve reaches a plateau at predetermined gelation time, and maximum adsorption level is reached. The gel content in the core at 1,7 days is shown in figure 6-11. The whole core has obtained the maximum gel capacity, which is shown in blue.

The gel concentration at 12 days was calculated to be $5{,}23 \cdot 10^{-4}$ kg/cm^3 (cf. Appendix 1), which gives a gel mass of $4{,}18 \cdot 10^{-2}$ kg for 1 pore volume. Net gel reacted from the simulation results was $6{,}25 \cdot 10^{-3}$ kg. The adsorbed mass of gel at 12 days was calculated to be $8{,}00 \cdot 10^{-5}$ kg, and the adsorbed gel mass from the simulation results were $8{,}02 \cdot 10^{-5}$ kg (cf. Appendix 1). The adsorbed gel mass corresponds well with the simulation results, but the net reacted gel from the simulation results does not match the calculated gel mass. This is because not all of the components are reacting. With the relative concentrations connected to each reacting component, a more accurate result can be obtained.

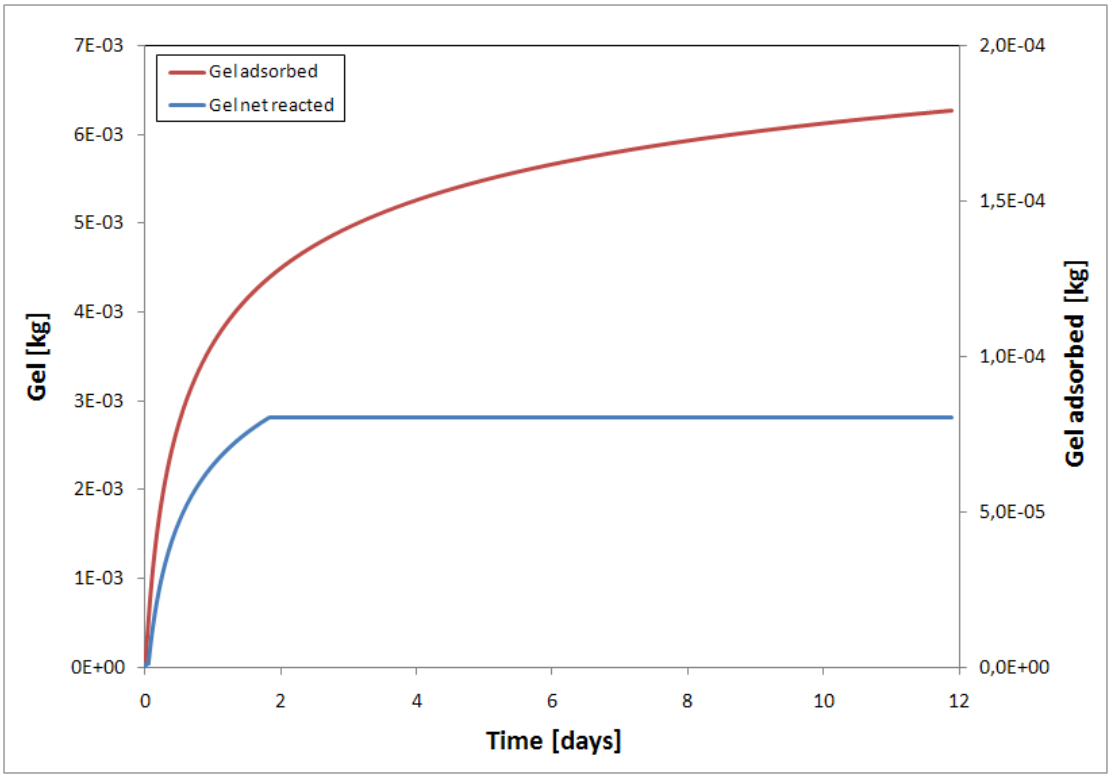

Figure 6-10: Gel concentration and adsorbed gel versus time.

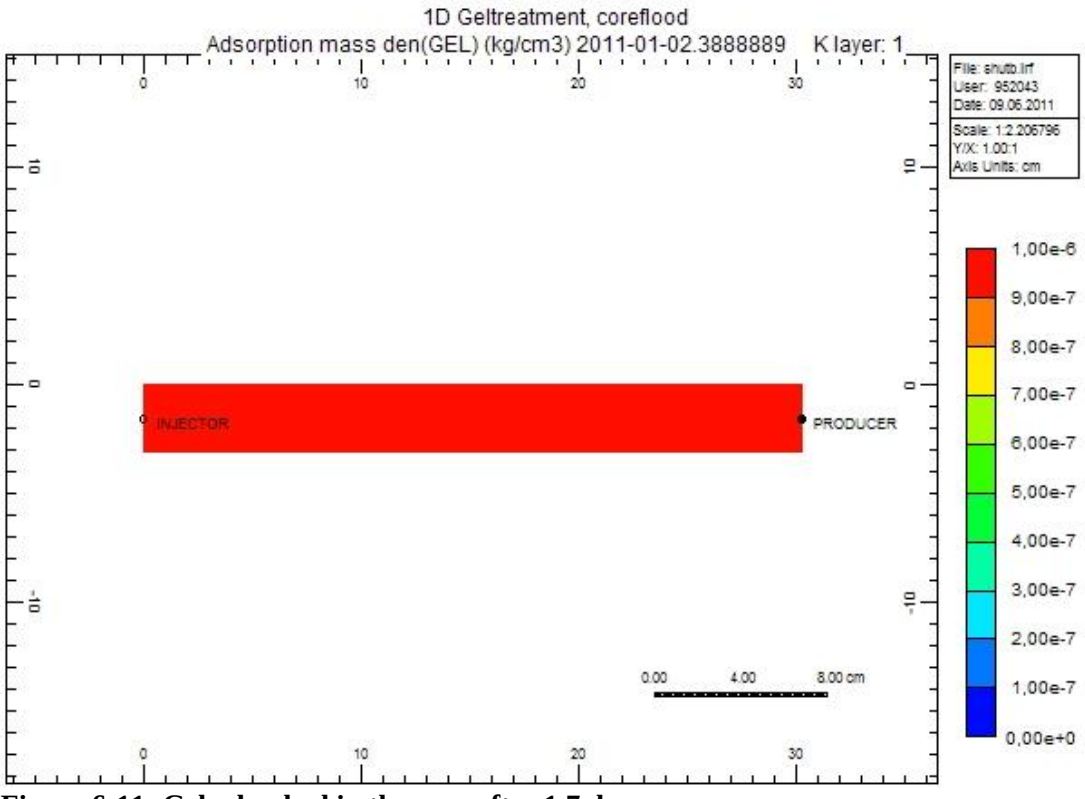

Figure 6-11: Gel adsorbed in the core after 1,7 days.

6.2.3 Post shut-in period (injection of water) – matching of *RRF*

After the shut-in period, water was injected with a injection rate of 0,05 ml/min. Figure 6-12 shows the *RRF* of the experiment, the model and simulated. The solid black line is the modelled *RRF*, the blue solid line is the experimental data and the red line is the *RRF* obtained from the simulation results. What happened during the experiment was that the water started to poke holes in the gel, which reduced the strength of the gel. Thereby, the *RRF* reduced significantly when the water started to flow through the gel, from 0 to 1 pore volumes fluid injected. After 1 pore volume fluid injected the water has broken through the gel. To match the experimental *RRF*, the *RRF* in the simulator has to be modified for each 0,1 pore volume, since STARS treats *RRF* as a constant. For the experimental RRF and the simulated *RRF*, *RRF* follows the trend of the pressure in figure 6-13. From 0 pore volumes to 0,22 pore volumes fluid injected, the adsorption of gel is set as reversible, since the gel is starting to rupture. The *ADRT* was set to 10% of *ADMAXT*. Thereby, a good match between the simulated *RRF* and the experimental *RRF* was obtained, connected the differential pressure. The difference in experimental and simulated differential pressure is around 100 mbar. After this period the adsorption was set as irreversible, i.e. *ADRT* equal to *ADMAXT*. For *RRF* equal to 5000 the differential pressure from the simulation follows the trend of the experimental data. At 1 pore volume fluid injected the differential pressure is around 0, which means that the gel is broken down. The *RRF* is 20 at this stage. To be able to match the experimental *RRF*, irreversible adsorption had to be used after 1 pore volume fluid injected, because issues with negative differential pressure. *ADRT* was set to 10% of *ADMAXT*. The *RRF* from the simulation results after 1 pore volume fluid injected is around 4,8, which corresponds well with the experimental *RRF* of 2,7.

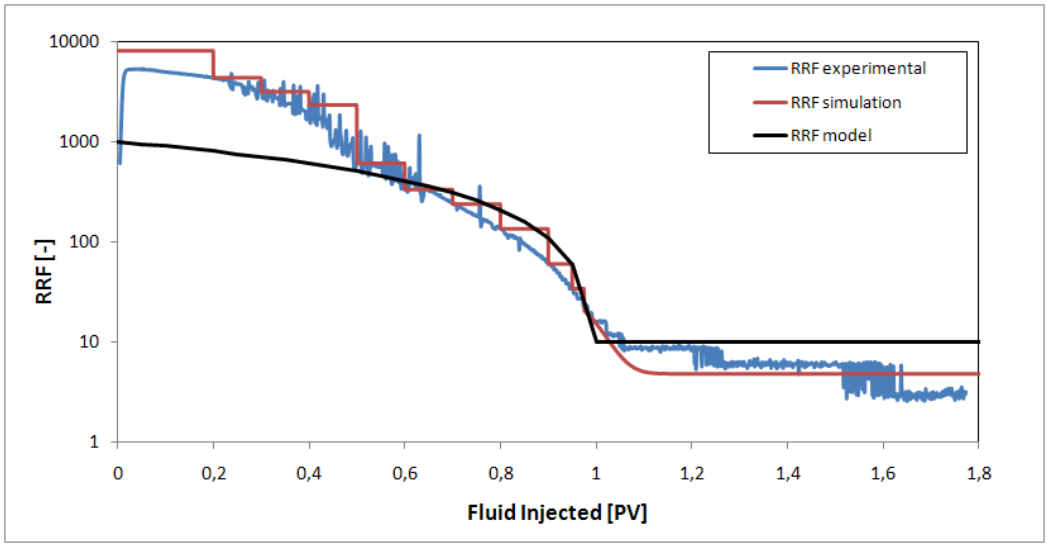

Figure 6-12: *RRF* versus water injected in post shut-in.

Overall, the simulated *RRF* matches well with the experimental data connected to the differential pressure. To obtain a good match with the experimental data at high and low *RRF*'s, the adsorption is set as reversible. For 5000 < *RRF* < 20, irreversible adsorption was used to match the experimental differential pressure.

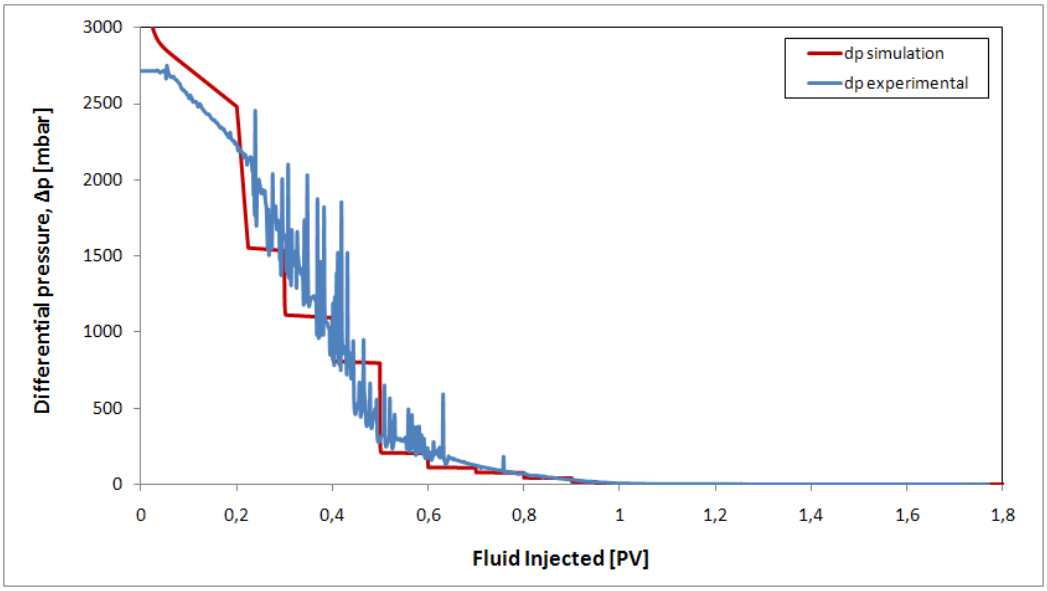

Figure 6-15: Differential pressure versus fluid injected, corresponding to the *RRF* in figure 6-14.

6.3 Dynamic versus Static coreflooding

Two different injection designs have been introduced, dynamic and static injection. By continuously injection of silicate solution, gel is formed at a preferred gelation time. By using a static injection method, a certain amount of silicate is injected, followed by a shut-in period to make the silicate solution gel.

First of all, dynamic injection requires much more silicate solution, compared to the static case, but the advantages are that more gel is created and which means that more of the pores are blocked. The net reacted gel mass can be calculated when the relative concentrations of the reacting components are known.

Static injection requires a shut-in period, so that the silicate solution gels. To get a successful gel treatment it is important that the shut-in time is long enough, in order to obtain sufficient strength of the gel.

The *RRF* from the dynamic coreflood experiment was 8000 and the *RRF* from the static coreflood was also approximately 8000, initially in the post shut-in period. Due to rapture of the gel, the *RRF* decreased rapidly afterwards. The degradation of gel can be simulated by using a reversible adsorption of gel at $RRF > 5000$ and $RRF < 20$. Otherwise an irreversible adsorption is used for gel.

6.4 Core versus reservoir scale

To get a successful gel treatment the most important factors is the gel strength, which depends on the gelation time and shut-in time. There is a large difference between gel treatment in core scale versus reservoir scale. In core scale it is mostly a linear flow, while on reservoir scale, the flow pattern varies from linear to radial flow. There is also variation in velocity.

However, the matching of the relative concentrations of the effluents are the most important, regarding converting from core to reservoir scale. By matching the relative concentration of the effluents in the experiment and form the simulation results, it is possible to observe when the silicate is starting to get adsorbed and when the gel is first getting formed.

Another important issue regarding the design of the gel is the depth of placement. When converting from core to reservoir scale it is important with a sufficient gel volume and the gelation time of the gel, to obtain sufficient gel strength at a desirable time. The reaction rate gives a good match at certain HCl concentrations. To get a better match of gelation times for other HCl values, the order of reaction and the frequency factor in the equation for reaction rate have to be tuned and matched with experimental data.

The effect of ions in the formation is not implemented in the simulation, but has to be considered, when designing the silicate solution for reservoir scale. Calcium is not involved in the chemical reaction in the simulation, but effects the gelation time due

to exchange of ions. The formation has to be pre-flushed to avoid precipitation of $Mg(OH)_2$, because of chemical reaction between reservoir minerals and sodium silicate.

When the reservoir model is increased in size, the number of grids is important regarding the accuracy of the simulation results. By increasing the number of grid blocks, a more accurate result is obtained. However, increasing the amount of grid blocks, the larger becomes the simulation time.

6.5 Model limitation

There are two factors that affect the result of the simulation. The first one is related to the chemical reaction. To create gel, a chemical reaction has to be defined, based on the injected components. In this case, the injected components beside water, is about 9-11% of the injected fluid. Not all of the injected components are converted to gel (cf. 6.1.1). Some water is also integrated in the gel structure (cf. 2.5), but it is not possible to implement water in the STARS chemical reaction.

On the other hand, the chemistry of silicate is complex, and the process in STARS is simplified by defining a simple chemical reaction. Hydrochloric acid is used to control the pH of the silicate solution, and is implemented in the chemical reaction. Since it is initially assumed that all of the components injected would eventually convert into gel, the gel concentration is much lower than predicted. Because of that, it is difficult to predict the gel concentration.

The gelation kinetics is not fully understood, since the model creates a significant amount of gel initially, while in reality the silicate solution would start to gel after a certain while. To deal with this issue a critical gelation time and critical gel concentration term is introduced, in order to make the model reach its maximum adsorption capacity at the predetermined gelation time.

The blocking mechanism in STARS can be adjusted in the adsorption data, by modifying the *RRF* or the level of adsorption. This deviates from the reality, since the *RRF* is based on the mobility of the fluid, and not the adsorption of gel. The gel is thereby formed and adsorbed to the rock, which will reduce the permeability of the rock. In reality the viscosity of the silicate solution increases to a point where it is too viscous to move and plug the pores. Also the increasing in molecular weight affects the gelation process, as it gets stuck in the pore throats. This is not taken into consideration in the model.

Conclusions

A simulation model has been developed, which can reproduce experimental data obtained from experiments performed at IRIS. Utilising the STARS simulator gel creation and behaviour modelling capabilities it is possible to simulate and match silicate gel treatment results observed from various experimental coreflood runs. More specifically two parameters, namely critical gel concentration and time are introduced, in order to obtain blocking effect at predetermined time.

Two injection methods were introduced, dynamic and static injection of silicate solution. It is simpler to predict the amount of gel created for static injection compared to dynamic injection.

In the dynamic coreflood the relative concentration of effluents from the simulation results matched the experimental data for the two first injection rates. A better match can be obtained by modifying the order of reaction for lower injection rates. The behaviour of calcium can be matched by implementing it in the chemical reaction.

The differential pressure obtained from the simulation matched well with the experimental in dynamic coreflood #3. To obtain the right differential pressure, the *RRF* has to be modified at plugging time. A *RRF* value of 8000 gives a good match with the experimental *RRF*.

The *RF* is mainly affected by the viscosity of the silicate solution when the residence time is lower than the designed gelation time. The simulation results correspond well with the experimental data.

In the post shut-in period, the *RRF* from the simulation results match well with the experimental data, connected to the differential pressure. For $5000 < RRF < 20$, irreversible adsorption was used to match the experimental differential pressure. Outside this range reversible adsorption was used, where *ADRT* was 10% of *ADMAXT*.

The reaction rate gives a good match at certain values for the amount of acid added to the silicate solution. To get a better match of gelation times for other HCl values, the order of reaction and the frequency factor in the equation for reaction rate have to be tuned and matched with experimental data. This is very important regarding field application.

Number of grids, molecular weight of silicate and adsorption data is important regarding the accuracy of the simulation results. By increasing the number of grid blocks, a more accurate result is obtained.

Recommendations for further work

Recommendations for the future would be to take the knowledge obtained by the modelling at micro-scale and convert it to field-scale. The behaviour of the gel can be studied and predicted at reservoir scale. By implement several layers in the reservoir model with unequal permeability and porosity data, parameters such as the effect of effect can be investigated.

References

Burns, L.D., Burns, M., Wilhite, P., McCool, S., Oglesby, K. and Glass, J. (2008) *New Generation Silicate Gel System for Casing Repairs and Water Shutoff*. SPE 113490 prepared for presentation at the 2008 SPE/DOE Improved Oil Recovery Symposium, Tulsa, Oklahoma, U.S.A, April 19-23.

Computer Modelling Group (CMG), http://www.cmgroup.com/software/stars.htm, Access date: 03/06-2011.

eCompond.com, http://www.ecompound.com/Reaction%20reference/reaction_workup_and_separation.htm, Access date: 28/5-11.

Grattoni, C.A., Jing, X.D. and Zimmerman, R.W. (2001) *Disproportionate Permeability Reduction When a Silicate Gel is Formed In-Situ to Control Water Production*. SPE 69534 prepared for presentation at the SPE Latin American and Caribbean Petroleum Engineering Conference, Buenos Aires, Argentina, March 25-28.

Green, D.W. and Willhite, P.G (1998) *Enhanced Oil Recovery.* SPE Textbook Series Volume 6. pages 143-154, 162.

Hatzignatiou, D.G. (2011), personal communication.

Herbas, J., Romero, M.F., Coombe, D. and Serna, A. (2004) *Gel performance Simulations and Laboratory/Field Studies to Design Water Conformance Treatments in Eastern Venezuelan HPHT Reservoirs*. SPE 89398 prepared for presentation at the 2004 SPE/DOE Fourteenth Symposium on Improved Oil Recovery, Tulsa, Oklahoma, U.S.A, April 17-21.

Herbas, Julio, Moreno, Raul, Marín, Amaurym Romero, María F. and Coombe, Dennis (2004) *Reservoir Simulation of Non Selective Placement of a Polymer Gel Treatment to Improve Water Injection Profiles and Weep Efficiency in the Lagomar Field Western Venezuela*. SPE 92025 prepared for presentation at the 2004 SPE International Petroleum Conference in Mexico, Puebla, Mexico, November 8-9.

Iler, R.K. (1979) *The Chemistry of Silica, Solubility, Polymerization, Colloid and surface Properties and Biochemistry*, John Wiley & Sons, pages 174-177.

Kabir, A.H. (2001) *Chemical Water & Gas Shutoff Technology – An Overview*. SPE 72119 prepared for presentation at the SPE Asia Pacific Improved Oil Recovery Conference, Kuala Lumpur, Malaysia, October 8-9.

Kennedy, H.T. (1936) *Chemical Methods for Shutting Off Water in Oil and Gas Wells*. AIME, Volume 118, pages 177-186.

Krumrine, P.H. and Boyce S.D. (1985) *Profile Modification and Water Control With Silica Gel-Based Systems*. SPE 13578 presented at the International Symposium on Oilfield and Geothermal Chemistry, Phoenix, Arizona, U.S.A, April 8-11.

Lakatos, I., Lakatos-Szabó, J., Tiszai, Gy., Palaásthy, Gy., Kosztin, B., Trömböczky, S., Bodola, M. and Patterman-Farkas, Gy. (1999) *Application of Silicate-Based Well Treatment Techniques at the Hungarian Oil Fields*. SPE 56739 prepared for presentation at the 1999 SPE Annual Technical Conference and Exhibition, Houston, Texas, U.S.A, October 3-6.

Lei, G., Li, L. and Nasr-El-Din, A. (2010) *New Gel Aggregates for Water Shut-off Treatments*. SPE 129960 prepared for for presentation at the 2010 SPE Improved Oil Recovery Symposium, Tulsa, Oklahoma, U.S.A. April 24-28.

Masterton, W.L and Hurley, C.N (2004) *Chemistry – Principles and Reactions*. Thomson Learning, pages 283-300.

Nabzar, L. Chauveteau, G. and Roque, C. (1996) *A New Model for Formation Damage by Particle Retention.* SPE 31119 prepared for presentation at the International Symposium on Formation Damage Control, Lafayette, Louisiana, U.S.A, Februray 14-15.

Rolfsvåg, T.A., Jakobsen, S.R., Lund, T.A.T. and Strømsvik, G. (1996) *Thin Gel Treatment of an Oil Producer at the Gullfaks Field: Results and Evaluation*. SPE 35548 prepared for presentation at the European Production Operations Conference & Exhibition, Stavanger, Norway, April 16-17.

Scott, T., Roberts, L.J., Sharpe, S.R., Clifford, P.J.and Sorbie, K.S. (1987) *In-Situ Gel Calculations in Complex Reservoir Systems Using a New Chemical Flood Simulator*. SPE 14234 presented at the 1985 SPE Annual Technical Conference and Exhibition, Las Vegas, U.S.A, September.

Schiozer, D.J. and Paulo, J. (2009) *Methodology to Compare Smart and Conventional Wells*. SPE 124949 prepared for presentation at the SPE Annual Technical Conference and Exhibition, New Orleans, Louisiana, U.S.A, October 4-7.

Schlumberger(2011),http://www.glossary.oilfield.slb.com/DisplayImage.cfm?ID=497 Access date: 28/05-2011.

STARS User's Manual, Version 2009.13, Computer Modelling Group (CMG), Calgary, Alberta, Canada, 2009.

Stavland, A. (2011), personal communication.

Stavland, A., Kvanvik, B.A. and Lohne, A. (1994) *Simulation Model for Predicting Placement of Gels*. SPE 28600 prepared for presentation at the SPE 69th Annual Technical Conference and Exhibition, New Orleans, LA, U.S.A, September 25-28.

Stavland, A., Jonsbråten, H.C. and Vikane, O. (2011) *In-Depth Water Diversion Using Sodium Silicate on Snorre – Factors Controlling In-Depth Placement*. SPE 143836 prepared for presentation at the SPE European Formation Damage Conference, Noordwjik, The Netherlands, June 7-10.

Stavland, A., Jonsbråten, H.C., Vikane, O., Skrettingland, K. and Fischer, H. (2011) *In-Depth Water Diversion Using Sodium Silicate – Preparation for single field pilot on Snorre*. Paper presented at the 16th European Symposium on Improved Oil Recovery, Cambridge, UK, April 12-14.

Sydansk, R.D. and Seright, R.S. (2006) *When and Where Relative Permeability Modification Water-Shutoff Treatments Can Be Successfully Applied*. SPE 99371 prepared for presentation at the 2006 SPE/DOE Symposium on Improved Oil Recovery, Tulsa, Oklahoma, U.S.A, April 22-26.

Vinot, B., Schecter, R.S and Lake, L.W. (1989) *Formation of Water-Soluble Silicate Gels by the Hydrolysis of a Diester of Dicarboxylic Acid Solubilized as Microemulsions*. SPE 14236 prepared for presentation at the 60th Annual Technical Conference and Exhibition of the SPE, Las Vegas, NV, September 22-25.

Nomenclature

μ_p: Silicate/polymer viscosity [cP]

μ_w: Water viscosity [cP]

λ_{after}: Mobility after DPR fluid flow [mD/cP]

λ_{before}: Mobility before DPR fluid flow [mD/cP]

ϕ_f: Fluid porosity [-]

ρ_j: Density [kg/cm^3]

A: Gelation time tuning parameter [-]

AD: Variable adsorption level obtained from the concentration [kg/(cm^3·PV)]

ADMAXT: Maximum adsorption capacity [kg/(cm^3·PV)]

ADRT: Residual adsorption level [kg/(cm^3·PV)]

ADSCOMP: Adsorption component

ADSTABLE: Denotes table of adsorption versus composition

Al^{3+}: Aluminium concentration [wt%]

Area: Cross-sectional area of core [cm^2]

C/C_0: Effluent concentration/initial concentration [-]

Ca^{2+}: Calcium concentration [ppm]

C_i: Concentrations of reactants [kg/cm^3]

$C_{cri,gel}$: Critical gel concentration [kg/cm^3]

C_{gel}: Gel concentration [kg/cm^3]

CMM: Molecular weight of component.

E_a: Activation energy [J/mole]

EACT: Activation energy [J/mole]

e_k: Order of reaction [-]

EOR: Enhanced oil recovery

FILENAMES: Name of input and output files

FREQFAC: Reaction frequency factor [1/min]

HCl: Hydrochloric acid concentration [wt%]

INCOMP WATER: Mass fractions of injected water phase [-]

IRIS: International Research Institute of Stavanger

k: Rate constant [1/min]

k_p : Effective polymer permeability [mD]

k_w : Effective water permeability [mD]

l : Length of core [cm]

MASSBASIS: Component property data is based on mass

m_{Gel} : Mass of gel [kg]

M_{wi} : Molecular mass of components [kg/gmol]

n: Ratio between SiO_2 and Na_2O

NCS: Norwegian Continental Shelf

PAM: Polyacrylamides

ppm: Part per million

PV: Pore volume [-]

q_{inj} : Injection rate [ml/min]

R: Molar gas constant [8,3145 J / (^oK·mole)]

RESTART: Time when to restart the simulation.

RF: Mobility reduction factor [-]

RF_d: Final mobility reduction [-]

RF_g: Initial mobility reduction [-]

r_k: Reaction rate [kg/(min·cm^3)]

RKW: Water phase permeability reduction factor [-]

RORDER: Order of reaction [-]

RPHASE: Defining phase for reacting component

RRF: Residual resistance factor [-]

RRF_d: Final permeability reduction [-]

RRF_g: Initial permeability reduction [-]

RRFT: Residual resistance factor for the adsorbing component [-]

r_{rk}: Frequency factor [1/min]

RXCRITCON: Critical value of reactants's concentration factor [-]

Si: Silicate concentration [wt%]

S_j: Saturation [-]

$sto1_{Al3+}$: Stoichiometric coefficient of aluminium [-]

$sto1_{Ca2+}$: Stoichiometric coefficient of calcium [-]

$sto1_{HCl}$: Stoichiometric coefficient of hydrochloric acid [-]

$sto1_i$: stoichiometric coefficient of reactants [-]

$sto1_{Si}$: Stoichiometric coefficient of silicate [-]

$sto2_{Gel}$: Stoichiometric coefficient of gel [-]

$sto2_i$: stoichiometric coefficient of products [-]

STOPROD: Stoichiometric coefficient of produced component

STOREAC: Stoichiometric coefficient of reacting component

T: Temperature [^oK]

$t_{cri,gel}$: Critical gelation time [min]

t_{gel}: Gelation time [days]

t_{res} : Residence time [min]

V_{pore} : Pore volume [ml]

w_{ji}: mass fraction of component i in phase j [-]

WRST: Frequency of writing the restart record.

WSO: Water shut-off

x: Relative front position of the degradation front [-]

α: Silicate dependent exponent, -0,6 [1/wt%]

β: Acid dependent exponent, -0,7 [1/wt%]

γ: Calcium dependent exponent, -0,1 [1/wt%]

Appendix 1

Dynamical coreflood experiment

Calculation of net reacted gel:

$$C_{gel} = \frac{t_{gel} \cdot r_{rk} \cdot (C_{HCl0} \cdot C_{HCl} / C_{HCl0})^3 \cdot (C_{Si0} \cdot C_{Si} / C_{Si0})^{0,1} \cdot (C_{Al0} \cdot C_{Al} / C_{Al0})^{0,1}}{e^{\frac{E_a}{R \cdot T}}}$$

$$C_{gel} = \frac{24hrs \cdot 60\,\text{min}/\,hrs \cdot 17days \cdot 6{,}15 \cdot 10^{19} 1/\,\text{min} \cdot [(1{,}30 \cdot 10^{-5} \cdot 0{,}75)^3 \cdot (1{,}30 \cdot 10^{-5} \cdot 0{,}75)^3 \cdot (1{,}30 \cdot 10^{-5} \cdot 0{,}75)^3] kg/cm^3}{e^{\frac{77000J/mole}{8{,}3145J/(^oK \cdot mole) \cdot 328{,}15^oK}}}$$

$$C_{gel} = 3{,}32 \cdot 10^{-5} kg/cm^3$$

Volume injected: 6 pore volumes

$m_{Gel} = 3{,}32 \cdot 10^{-5}$ kg/cm^3 $\cdot 6 \cdot$ 700 ml = 0,14 kg

Calculation of adsorbed gel:

Pore volume = 700 ml

$$m_{Gel,adsorbed} = ADMAXT \cdot V_{pore}$$

$$m_{Gel,adsorbed} = 2{,}00 \cdot 10^{-5} kg/cm^3 \cdot 700ml = 1{,}40 \cdot 10^{-2} kg$$

Static coreflood experiment

Calculation of net reacted gel:

$$C_{gel} = \frac{t_{gel} . r_{rk} \cdot \prod_{i=1}^{n_c} C_i^{e_k}}{e^{\frac{E_a}{R \cdot T}}} = \frac{t_{gel} . r_{rk} \cdot C_{HCl}^{4} \cdot C_{Si}^{0,1} \cdot C_{Al}^{0,1}}{e^{\frac{E_a}{R \cdot T}}}$$

$$C_{gel} = \frac{24 hrs \cdot 60 \min / hrs \cdot 12 days \cdot 1,85 \cdot 10^{25} 1 / \min \cdot [(2,21 \cdot 10^{-5})^4 \cdot (7,80 \cdot 10^{-6})^{0,1} \cdot (8,06 \cdot 10^{-9})^{0,1}] kg / cm^3}{e^{\frac{77000 J / mole}{8,3145 J / (^o K \cdot mole) \cdot 313,15^o K}}}$$

$$C_{gel} = 5,23 \cdot 10^{-5} kg / cm^3$$

Calculation of adsorbed gel:

Pore volume = 80 ml

$$m_{Gel,adsorbed} = ADMAXT \cdot V_{pore}$$

$$m_{Gel,adsorbed} = 1,00 \cdot 10^{-6} kg / cm^3 \cdot 80 ml = 8,00 \cdot 10^{-4} kg$$

Appendix 2

Calculation of gelation time for static coreflood:

$$t_{gel} = A \cdot e^{\alpha[Si]} \cdot e^{\beta[HCl]} \cdot e^{\gamma[Ca^{2+}]} \cdot e^{\frac{E_a}{RT}}$$

$$t_{gel} = 8,75 \cdot 10^{-10} \cdot e^{-0,6[3,0]} \cdot e^{-0,7[8,5]} \cdot e^{-0,1[20]} \cdot e^{\frac{77000\,J/mole}{8,314\,J/(^{o}K \cdot mole) \cdot (40+273,15)^{o}K}} days$$

$$t_{gel} = 1,7 days$$

Appendix 3

Calculation of reaction rate connected to each injection rate for dynamic coreflood:

q_{inj} = 11,7 ml/min:

2,2 pore volumes fluid injected on 0,04 days:

$$r_k = \frac{2,65 \cdot 10^{-3} kg}{131,5 \min \cdot 1538 cm^3} = 1,31 \cdot 10^{-8} \frac{kg}{\min \cdot cm^3}$$

q_{inj} = 0,4 ml/min:

1,5 pore volumes fluid injected in 1,18 days:

$$r_k = \frac{3,18 \cdot 10^{-2} kg}{2618,9 \min \cdot 1040 cm^3} = 1,17 \cdot 10^{-8} \frac{kg}{\min \cdot cm^3}$$

q_{inj} = 0,098 ml/min:

1,1 pore volumes fluid injected in 3,73 days:

$$r_k = \frac{3,26 \cdot 10^{-2} kg}{7639,2 \min \cdot 744 cm^3} = 5,91 \cdot 10^{-9} \frac{kg}{\min \cdot cm^3}$$

q_{inj} = 0,028 ml/min:

1,2 pore volumes fluid injected in 12,25 days:

$$r_k = \frac{4,63 \cdot 10^{-2} kg}{17640,0 \min \cdot 842 cm^3} = 3,12 \cdot 10^{-9} \frac{kg}{\min \cdot cm^3}$$

Appendix 4

Calculation of r_{rk} for dynamic coreflood:

Given that 100% of the injected components are reacting to gel:

$$r_{rk} = \frac{C_{gel} \cdot e^{\frac{Ea}{RT}} \cdot \prod_{i=1}^{n_c} C_i^{-e_k}}{t_{gel}}$$

$$r_{rk} = \frac{8{,}76 \cdot 10^{-5}\, kg/cm^3 \cdot e^{\frac{77000\, J/mole}{8{,}3145\, J/(^{o}\mathrm{K} \cdot \mathrm{mole}) \cdot 328{,}15^{o}\mathrm{K}}} \cdot [(1{,}30 \cdot 10^{-5})^3 \cdot (1{,}64 \cdot 10^{-5})^{0{,}1} \cdot (1{,}27 \cdot 10^{-8})^{0{,}1}]\, cm^3/kg}{13{,}6\, days \cdot 24\, hrs/days \cdot 60\, \mathrm{min}/hrs}$$

$$r_{rk} = 6{,}15 \cdot 10^{19} 1/\mathrm{min}$$